

CALIFORNIA CURRENT INTEGRATED ECOSYSTEM ASSESSMENT (CCIEA) CALIFORNIA CURRENT ECOSYSTEM STATUS REPORT, 2018

A report of the NOAA CCIEA Team to the Pacific Fishery Management Council, March 9, 2018.

*Editors: Dr. Chris Harvey (NWFSC), Dr. Toby Garfield (SWFSC), Mr. Greg Williams (PSMFC),
Dr. Nick Tolimieri (NWFSC), and Dr. Elliott Hazen (SWFSC)*

1 INTRODUCTION

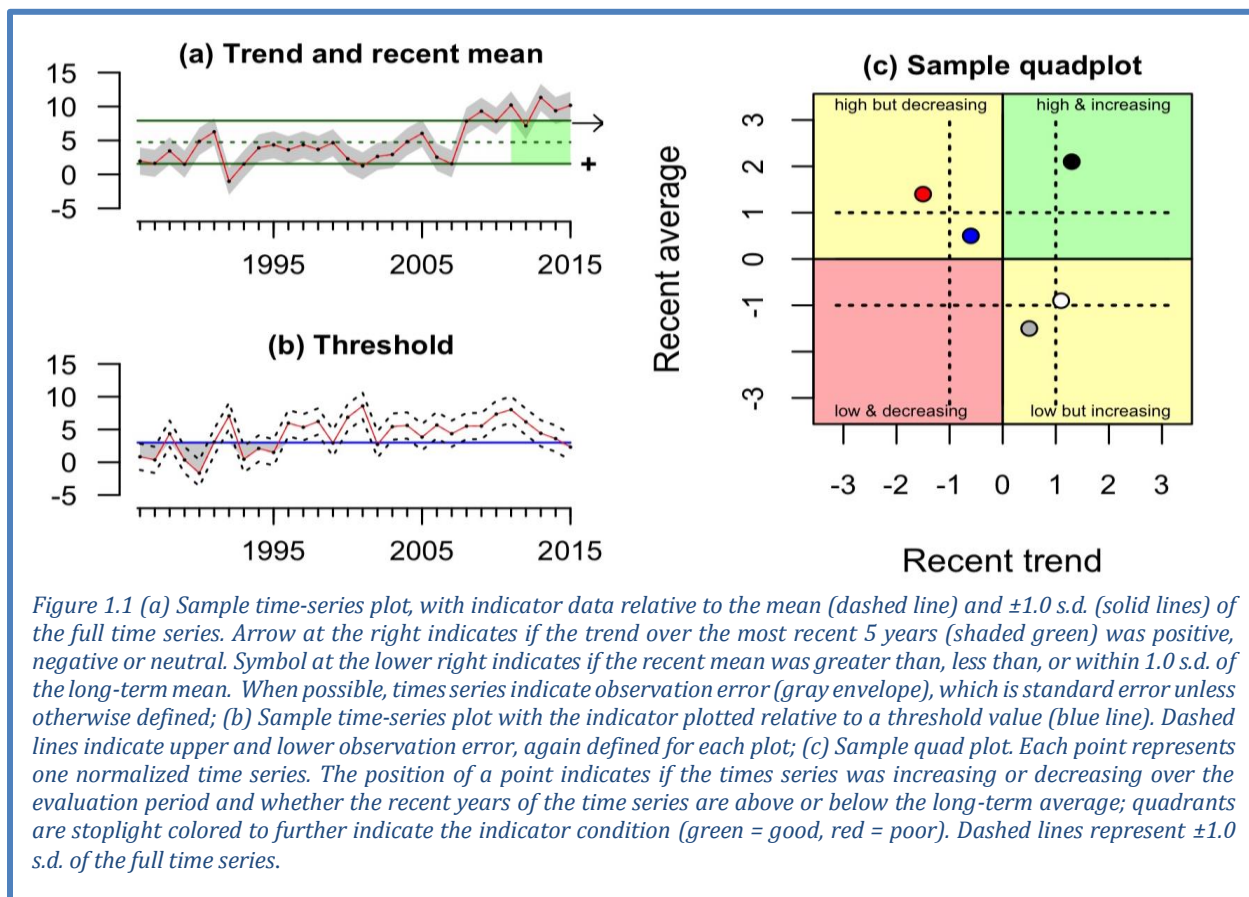
Section 1.4 of the 2013 Fishery Ecosystem Plan (FEP) established a reporting process wherein NOAA provides the Council with a yearly update on the state of the California Current Ecosystem (CCE), as derived from environmental, biological and socio-economic indicators. NOAA's California Current Integrated Ecosystem Assessment (CCIEA) team is responsible for this report. This marks our 6th report, with prior reports in 2012 and 2014-2017.

The highlights of this report are summarized in Box 1.1. Sections below provide greater detail. In addition, Supplemental Materials are provided at the end of this document, in response to previous requests from Council members or the Scientific and Statistical Committee (SSC) to provide additional information, or to clarify details found within this report.

Box 1.1: Highlights of this report

- **Climate, oceanographic and streamflow indicators suggest that the physical system is transitioning toward average or even La Niña conditions, following the marine heat wave (“Blob”) and major El Niño events of 2014-2016**
- **Several ecological indicators in 2017 also point toward more average conditions:**
 - The copepod community off Newport saw an increase in cool-water, lipid-rich species that are better for production of salmon
 - Some important forage species increased in the central and southern CCE
 - Sea lion pup growth at San Miguel Island was normal
 - There were no mass seabird mortality events
- **However, there was lingering evidence of unfavorable conditions in 2017:**
 - Persistent deep warm water remains in the northern portion of the system
 - Pyrosomes (warm-water salps) were extremely abundant in the northern and central CCE
 - Juvenile salmon catches were poor, and other indicators suggest that Chinook and coho salmon returns to the Columbia Basin will be below average in 2018
 - A major hypoxic event occurred on the shelf of the northern CCE in August-September
 - Reports of whale entanglements in fixed fishing gear were high for the fourth straight year; most reports involved crab gear, but some involved sablefish gear
- **For the first time, the report includes highly migratory species indicators, related to biomass, recruitment, and management of protected species bycatch**
- **Social vulnerability can now be compared with the dependence of coastal communities on commercial fishing and on recreational fishing**
- **We find some evidence of threshold relationships (between sea lions and upwelling), but no support yet for an “early warning index” of major ecosystem state changes**

Throughout this report, most time series figures follow common formats, illustrated in Figure 1.1. In coming years we will include model fits to time-series data, as recommended by the SSC Ecosystem Subcommittee (SSCES; see advisory body reports, Agenda Item E.1.b., March 2015).



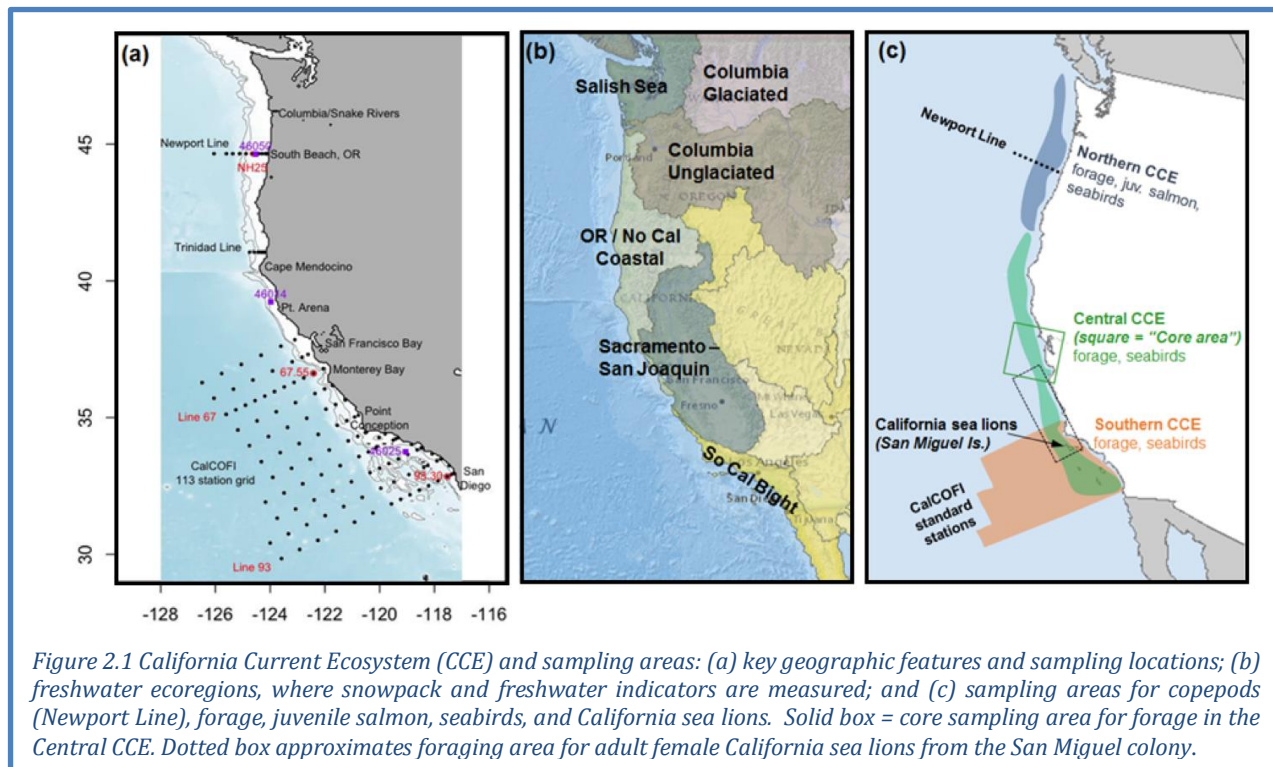
2 SAMPLING LOCATIONS

Figure 2.1 shows the CCE and headlands that define key biogeographic boundaries. We generally consider areas north of Cape Mendocino to be the “Northern CCE,” areas between Cape Mendocino and Point Conception the “Central CCE,” and areas south of Point Conception the “Southern CCE.”

Figure 2.1 also shows sampling locations for most regional oceanographic data in this report (Section 3.2). Much of the oceanographic data are collected on the Newport Line off Oregon and the CalCOFI grid off California. This sampling is complemented by basin-scale observations and models.

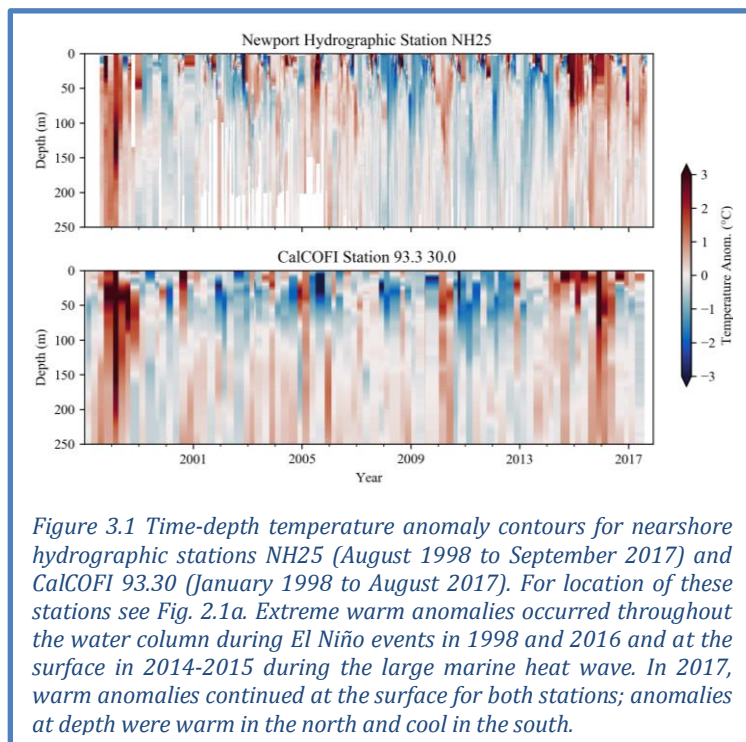
Freshwater habitats worldwide can be spatially grouped into “ecoregions” by Abell et al. (2008) (see also www.feow.org). Freshwater ecoregions in the CCE are shown in Figure 2.1b, and are the basis by which we summarize indicators for snowpack, streamflow and stream temperature (Section 3.4).

Shaded areas in Figure 2.1c indicate sampling locations for most biological indicators, including copepods (Section 4.1), forage species (Section 4.2), juvenile salmon (Section 4.3), California sea lions (Section 4.6) and seabirds (Section 4.7). The blue and green areas in Figure 2.1c also approximate the areal extent of the groundfish bottom trawl survey (Section 4.4), which covers trawlable habitat on the shelf and upper slope (55–1280 m depths) in US waters.



3 CLIMATE AND OCEAN DRIVERS

Climate and ocean indicators in the CCE reveal a climate system still in transition in 2017. The historically unprecedented marine heat wave in the CCE from 2014-2016 and the strong El Niño event in the tropical Pacific in the winter of 2015-2016 gave way to cooler coastal waters, a succession of strong storms in the winter of 2016-2017, and weak La Niña conditions by late 2017. The transition is visible in Figure 3.1 at right, where the deep and persistent red bands of above-average water temperatures from 2014-2016 return to more average or cool conditions in 2017 at the far right. We continued to see deep residual warm water and associated species from the warming events, especially in the north (Figure 3.1, top), but basin-scale indicators are trending toward average or cooler conditions. As described below, regional indicators of upwelling, water chemistry and stream conditions demonstrated their characteristically high spatiotemporal variability.



3.1 BASIN-SCALE INDICATORS

Atmosphere-ocean energy exchange is a major driver of CCE dynamics at multiple temporal and

spatial scales. To capture large-scale physical variability, the CCIEA team reports three independently varying indices capable of producing a wide range of potential ecosystem states. The Oceanic Niño Index (ONI) describes the equatorial El Niño Southern Oscillation (ENSO). A positive ONI indicates El Niño conditions, which usually mean more storms to the south, weaker upwelling, increased poleward transport of equatorial waters (and species), and lower primary productivity in the CCE. A negative ONI means La Niña conditions, which usually lead to higher productivity. The Pacific Decadal Oscillation (PDO) is derived from sea surface temperature anomalies (SSTa) in the Northeast Pacific, which often persist in regimes that last for many years. Positive PDOs are associated with warmer waters and lower productivity in the CCE, while negative PDOs are associated with cooler waters and higher productivity. The North Pacific Gyre Oscillation (NPGO) is a low-frequency signal of sea surface height, indicating changes in the circulation of the North Pacific Subtropical Gyre and Alaskan Gyre, which in turn relate to the source waters for the CCE. Positive NPGO values are associated with increased equatorward flow and increases in surface salinities, nutrients, and chlorophyll-*a*. Negative NPGO values are associated with decreases in such values, less subarctic source water, and lower productivity.

In 2017, the ONI was neutral for a majority of the year, but shifted to weak La Niña conditions in October and November (Figure 3.1.1, top). La Niña conditions are forecast to continue into the summer of 2018. PDO values were positive but declining over the course of 2017, nearing the long-term mean for the first time since winter of 2013-2014 (Figure 3.1.1, middle). NPGO values ranged between neutral and negative, with the October 2017 value being the lowest of the year (Figure 3.1.1, bottom). The ONI and PDO indices suggest a return to conditions of higher productivity following the major El Niño of 2015-2016 and the large marine heat wave, a.k.a. “the Blob” (Bond et al. 2015) of 2013-2016. However,

while the Blob dissipated in fall of 2016, some slightly (<1 s.d.) anomalously warm surface water remained in the Gulf of Alaska and immediately along the West Coast in early 2017 (Figure 3.1.2, upper left). Summer SSTa generally increased, with some anomalies >1 s.d. off California and Baja California, and a negative SSTa near Cape Blanco (Figure 3.1.2, lower left). The influence of the large marine heat wave and 2016 El Niño event are especially evident in the 5-year means (Figure 3.1.2, middle) with positive anomalies in the Gulf of Alaska in the winter and expanding to the majority of the domain by the summer. The 5-year trends for SSTa are negative in the west during the winter and closer to the coast during the summer (Figure 3.1.2, right); these negative trends are a result of cooler temperatures in 2016-17 following the highs of 2014-15.

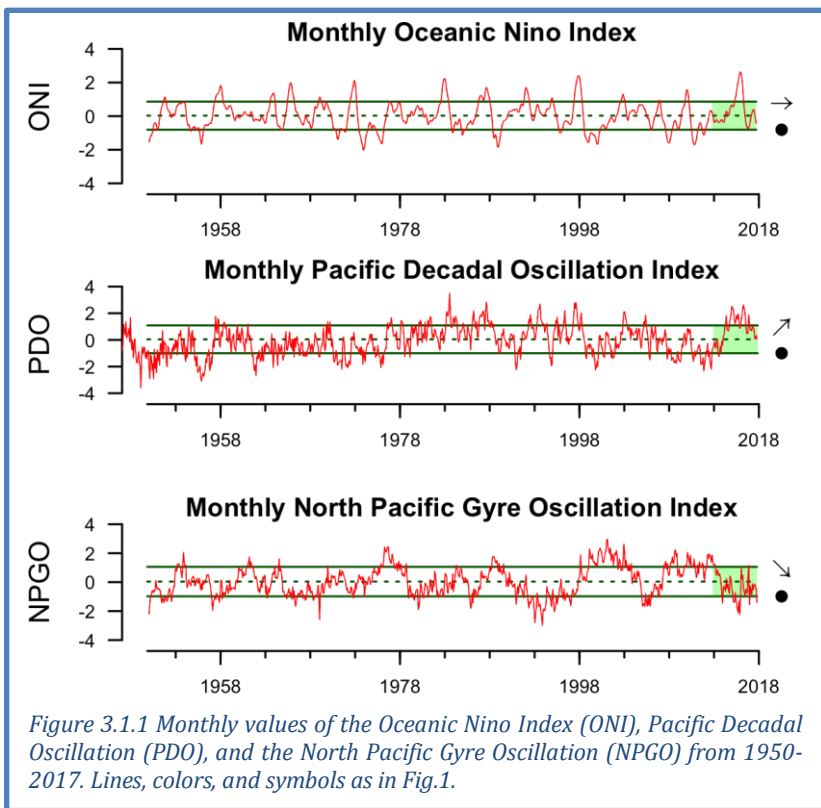
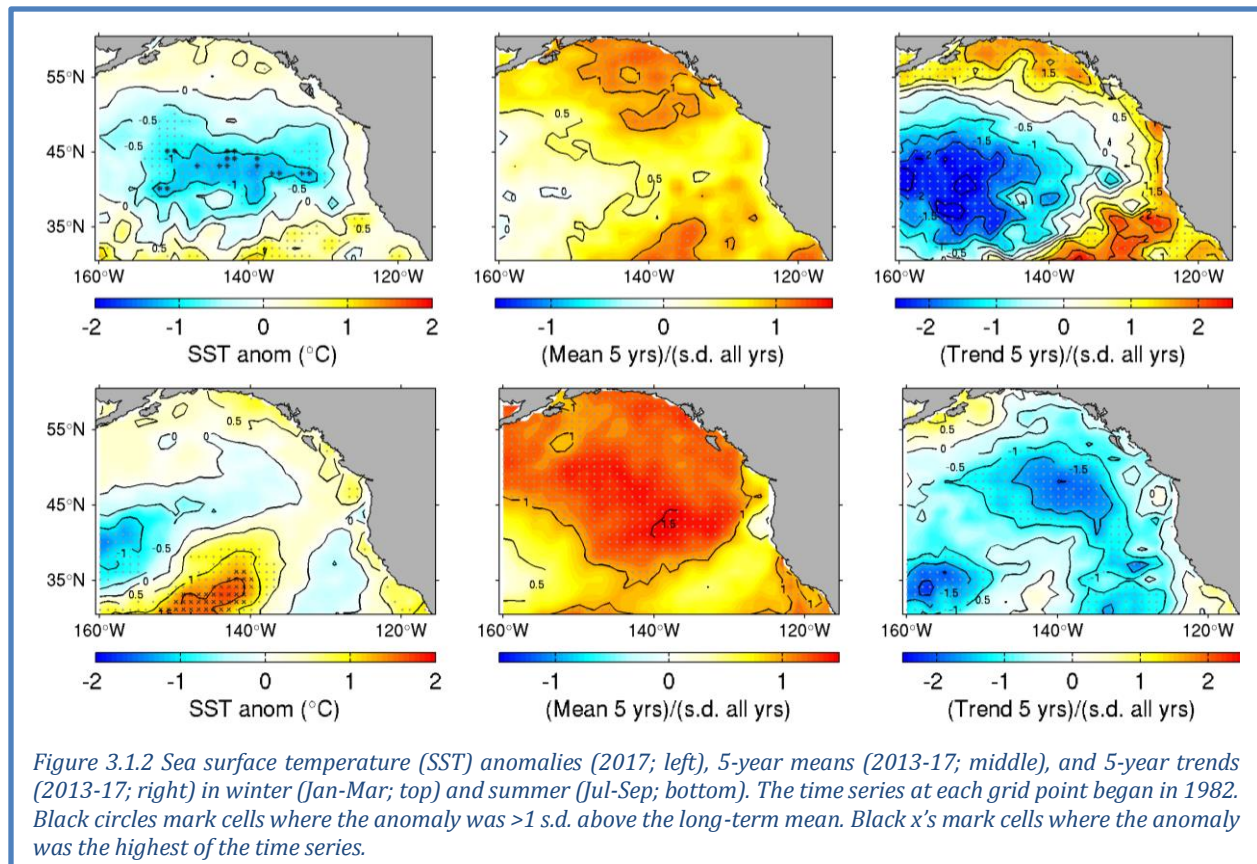


Figure 3.1.1 Monthly values of the Oceanic Niño Index (ONI), Pacific Decadal Oscillation (PDO), and the North Pacific Gyre Oscillation (NPGO) from 1950-2017. Lines, colors, and symbols as in Fig.1.



In summary, while the large marine heat wave and 2015-16 El Niño event brought warm waters and associated warm water species (Barceló et al. 2017, Santora et al. 2017), temperatures moderated during 2017 and basin-scale indices are returning to neutral or La Niña conditions. However, the cooler coastal waters in the northern CCE are largely surface-oriented, with the subsurface showing lingering signs of the recent warming events (Figure 3.1). Thorough summaries of these dynamics are in Leising et al. (2015), McClatchie et al. (2016), and Wells et al. (2017). These large-scale forces will help explain the dynamics of biological indicators in Section 4 below.

3.2 REGIONAL CLIMATE INDICATORS

Seasonal high pressure over the Gulf of Alaska and low pressure over the US Southwest produce the northerly alongshore winds that drive coastal upwelling in the CCE. Upwelling is a physical process of moving cold, nutrient-rich water from deep in the ocean to the surface, which fuels the high seasonal primary production at the base of the CCE food web. The most common metric of upwelling is the Bakun Upwelling Index (UI), derived from the US Navy Fleet Numerical Meteorology and Oceanography Center's sea level pressure product, reported at a spatial scale of 1° latitude x 1° longitude. The timing, strength, and duration of upwelling vary greatly in space and time. The cumulative upwelling index (CUI) is one way to summarize this variability at a given location over the course of a year. CUI integrates the onset of upwelling favorable winds ("spring transition"), a general indication of the strength of upwelling, relaxation events and the end of the upwelling season.

Upwelling displayed significant regional variability in 2017, with the least favorable conditions in the northern CCE (Figure 3.2.1, Appendix E, Figure E.2.1). At 45° N (near Newport, OR), average downwelling from January to April was followed by average upwelling from May to July; CUI through April was much higher than 2016, but lower than 2015, which featured strong winter upwelling (Figure 3.2.1; Appendix E, Figure E.2.1). At 39° N (near Point Arena), there was a late spring transition

date in March and very little upwelling until the beginning of June, when a period of strong upwelling began that lasted until October. In the Southern California Bight (~33° N), CUI was average until April, and above average from May onward, although the Bakun UI performs poorly in this region due to the south-facing shore and complex topography.

Over the last 5 years, CUI has been below-average in the northern CCE and average to above-average in the central and southern CCE (Appendix E, Figure E.2.1). Thus, even as basin-scale indices were returning to average conditions in 2017, regional differences in upwelling may help explain why surveys found regional differences in temperature anomalies and productivity. In particular, the northern CCE experienced residual warm water (Figure 3.1), below-average chlorophyll-*a* (Wells et al. 2017), and lagging ecological conditions as described in Section 4.

3.3 HYPOXIA AND OCEAN ACIDIFICATION

Nearshore dissolved oxygen (DO) is dependent on many processes, including currents, upwelling, air-sea exchange, and community-level production and respiration. Low DO can compress habitat and cause stress or die-offs for sensitive species. Waters with DO levels <1.4 ml/L (2 mg/L) are considered to be hypoxic.

Low DO was a serious issue in the northern CCE in 2017. At station NH05 (5 km off of Newport, OR), water near bottom over the continental shelf was below the hypoxia threshold from late July until early September (Figure 3.3.1, top) before its seasonal rebound in fall. Though perhaps not evident from the time series, this hypoxic event was among the most serious and spatially extensive observed in the northern CCE, causing widespread die-offs of crabs and other benthic invertebrates. The primary cause is thought to be upwelled deep ocean water that was more hypoxic than normal (F. Chan, Oregon State University, pers. comm.). Seasonal trends for these stations and other stations off Southern California (where DO was well above the 1.4 ml/L threshold) are shown in Appendix E.3.

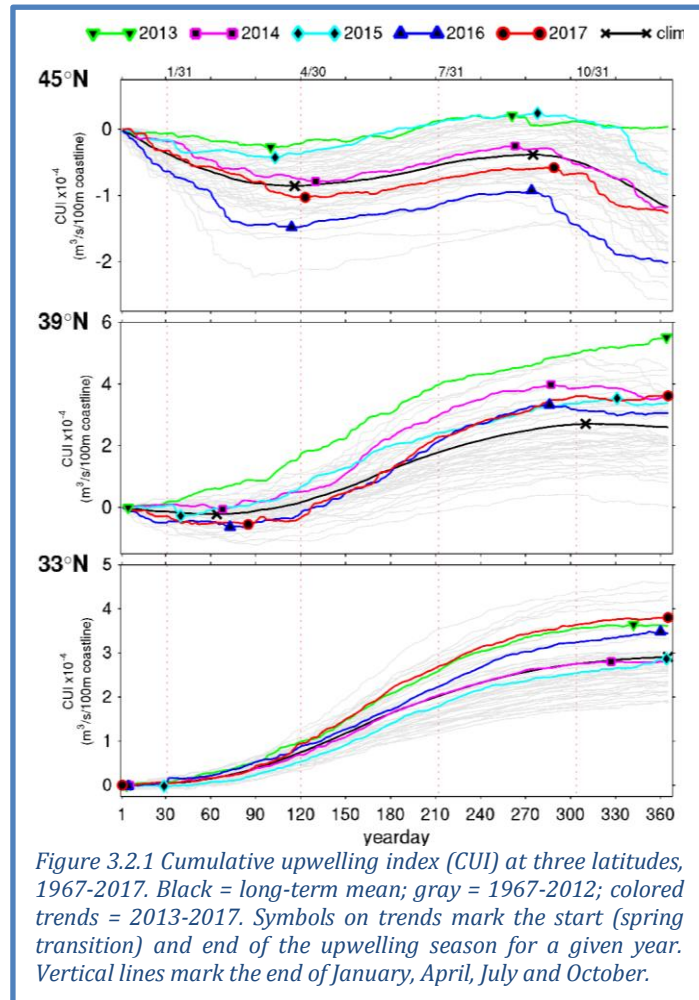


Figure 3.2.1 Cumulative upwelling index (CUI) at three latitudes, 1967-2017. Black = long-term mean; gray = 1967-2012; colored trends = 2013-2017. Symbols on trends mark the start (spring transition) and end of the upwelling season for a given year. Vertical lines mark the end of January, April, July and October.

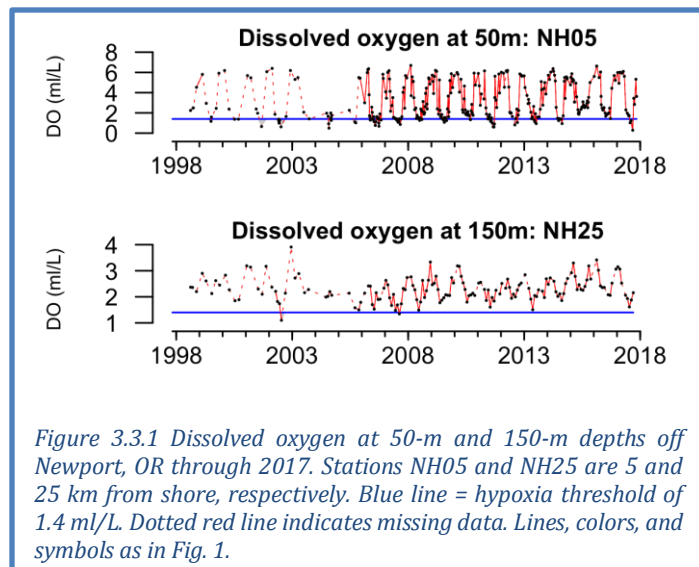


Figure 3.3.1 Dissolved oxygen at 50-m and 150-m depths off Newport, OR through 2017. Stations NH05 and NH25 are 5 and 25 km from shore, respectively. Blue line = hypoxia threshold of 1.4 ml/L. Dotted red line indicates missing data. Lines, colors, and symbols as in Fig. 1.

Ocean acidification (OA), caused by increased levels of atmospheric CO₂, reduces pH and carbonate levels in seawater. A key indicator of OA is aragonite saturation state, a measure of availability of aragonite (a form of calcium carbonate). Aragonite saturation <1.0 indicates corrosive conditions that may be stressful to shell-forming organisms. Upwelling, which drives primary production in the CCE, also transports hypoxic, acidified waters from offshore onto the continental shelf, where increased community-level metabolic activity can further exacerbate OA (Chan et al. 2008, Feely et al. 2008).

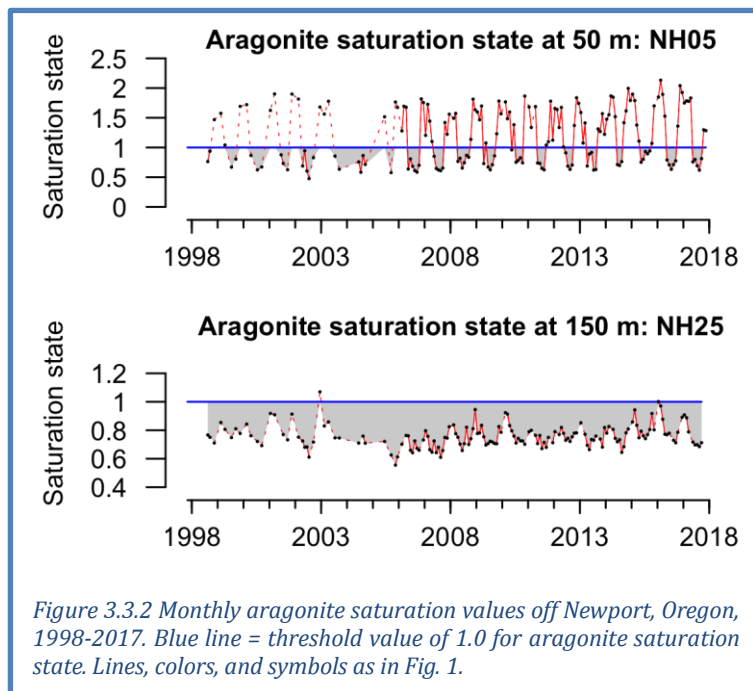


Figure 3.3.2 Monthly aragonite saturation values off Newport, Oregon, 1998-2017. Blue line = threshold value of 1.0 for aragonite saturation state. Lines, colors, and symbols as in Fig. 1.

Aragonite saturation levels off Newport in 2017 were fairly typical, and lower than in the anomalous

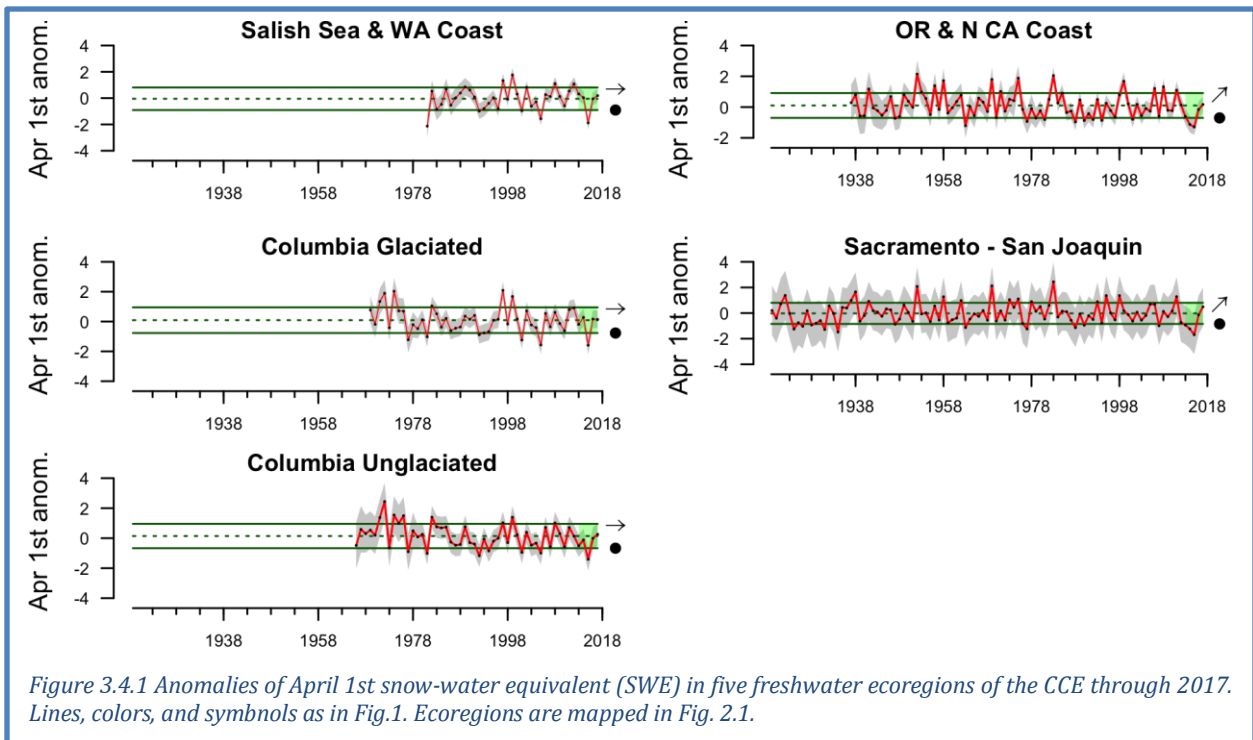
years of 2014-2015 (Figure 3.3.2). At the nearshore station (NH05), aragonite levels at 50 m depth were saturated (>1.0) in winter and spring, then fell below 1.0 in the summer and fall, as is typical, although corrosive water was shallower in summer-fall of 2017 than in recent years, possibly related to upwelling (Appendix E.3, Figure E.3.5). At station NH25 at 150 m depths, aragonite saturation state followed the same seasonal cycle but across a narrower range; conditions at this site and depth were almost always corrosive (<1.0). Seasonal aragonite trends are shown in Appendix E.3

3.4 HYDROLOGIC INDICATORS

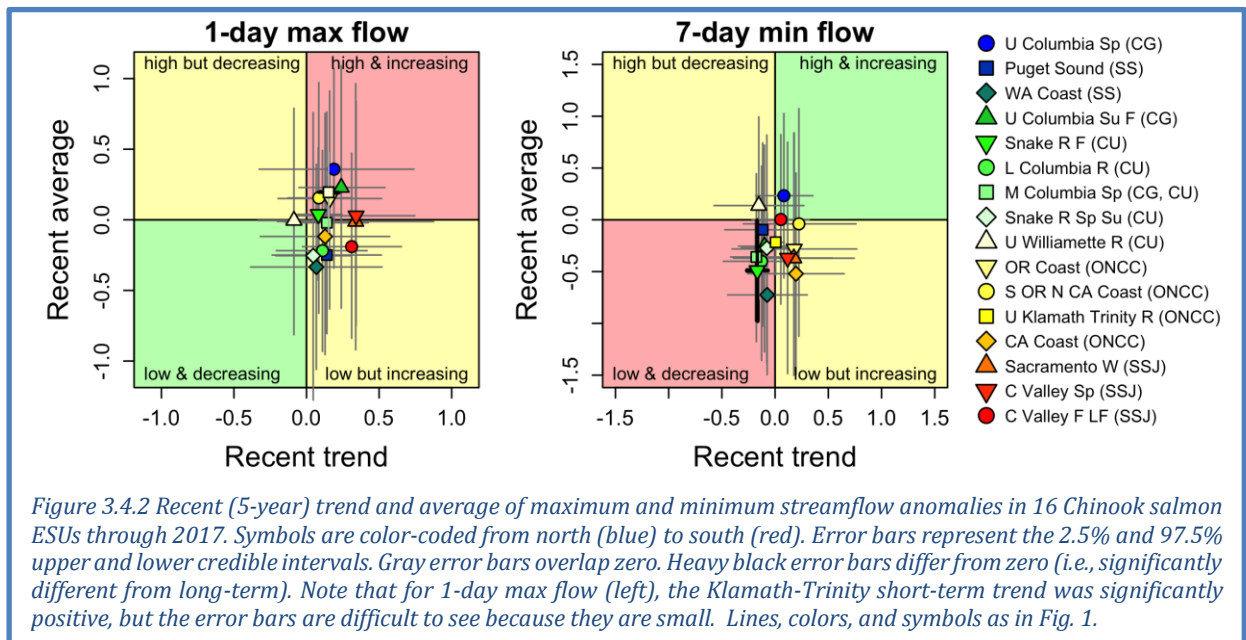
Freshwater conditions are critical for salmon populations and estuaries that support many marine species (e.g., Appendix D). The freshwater indicators presented here focus on salmon habitat conditions as related to snowpack, streamflow and temperature. Indicators are summarized by freshwater ecoregion (see Figure 2.1b) or, where possible, by salmon evolutionarily significant units (ESUs, sensu Waples 1995). Snow-water equivalent (SWE) is the water content in snowpack, which provides freshwater in the spring, summer and fall months. Maximum streamflow in winter and spring is important for habitat formation and removal of parasites, but extreme discharge can scour salmon nests (redds). Minimum streamflow in summer and fall can restrict habitat for in-stream juveniles and migrating adults. High summer water temperatures can impair physiology and cause mortality to both juveniles and adults. All indicators are influenced by climate and weather patterns and will be affected as climate change intensifies.

As in 2016, SWE in 2017 was consistent with long-term average levels in all ecoregions, after years of steady declines and the historic low of 2015 (Figure 3.4.1). As of January 1st, SWE in 2018 is on pace to be lower than 2017, particularly in the southern Cascade Range and the Sierra Nevadas (Appendix F). However, SWE values do not typically peak until around April 1 and may be greatly influenced by precipitation until then. Thus the official measure of SWE for the year will not be until April 1, 2018.

The relatively average SWE in 2017 resulted in maximum and minimum flows that were both well within the typical historical ranges at ecoregional scales (Appendix F). We summarized streamflow with quad plots that compile recent flow anomalies at the finer spatial scale of individual Chinook



salmon ESUs. Here, high and increasing maximum flows are regarded as undesirable (i.e., red quadrant of the max flow plot, Figure 3.4.2) due to redd scouring, while low and decreasing minimum flows are also undesirable (red quadrant of the min flow plot) because of the potential for stress related to temperature, oxygen, or space. The error bars describe 95% credible intervals of river flow, allowing us to determine which ESUs have short-term trends or status strongly greater than zero or the long-term mean, respectively. Maximum flow events were generally within range of long-term means and lacked strong trends, although the short-term trend for Klamath-Trinity was strongly positive (Figure 3.4.2, left). Minimum flow anomalies had worsening trends for just one ESU, Snake River fall run, which was strongly lower in both recent trend and recent average (Figure 3.4.2, right).



This year we added a new freshwater indicator, maximum August stream temperature, which is summarized in Appendix F. Most ecoregions in 2017 experienced maximum stream temperatures similar to historical averages, although the recent average for Salish Sea and Washington Coast streams was above the long-term mean. Long-term increases (0.01-0.04 °C/yr) in maximum August temperature starting in the 1980s and 1990s are evident in at least three ecoregions.

4 FOCAL COMPONENTS OF ECOLOGICAL INTEGRITY

The CCIEA team examines many indicators related to the abundance and condition of key species and the dynamics of ecological interactions and community structure. Many CCE species and processes respond quickly to changes in ocean and climate drivers, while other responses may not manifest for many years. These dynamics are challenging to predict. Between 2014 and 2016, many ecological metrics indicated conditions of poor productivity at lower trophic levels and poor foraging conditions for many predators. In 2017 we continued to observe unexpected community structure and remnants of the recent warm anomalies in pelagic waters throughout the CCE. However, some indicators described below suggest that ecological conditions are trending toward average conditions in parts of the CCE. It remains to be seen how some species and life history strategies were ultimately affected by the period of low productivity, or whether 2018 will represent a further shift toward average or above-average productivity.

4.1 NORTHERN COPEPOD BIOMASS ANOMALY

Copepod biomass anomalies represent inter-annual variation for two groups of copepod taxa: northern copepods, which are cold-water species rich in wax esters and fatty acids that appear to be essential for pelagic fishes; and southern copepods, which are warm-water species that are smaller and have lower fat content and nutritional quality. In summer, northern copepods usually dominate the coastal zooplankton community observed along the Newport Line (Figure 2.1a,c), while Southern copepods dominate during winter. El Niño events and positive PDO regimes can promote higher biomass of southern copepods (Keister et al. 2011, Fisher et al. 2015). Threshold values for the anomalies have not been set, but positive values of northern copepods in summer are correlated with stronger returns of Chinook salmon to Bonneville Dam, and values >0.2 are associated with better survival of coho salmon (Peterson et al. 2014).

From the start of the anomalous warm period in fall 2014 until spring 2017, copepod anomaly trends strongly favored southern copepods. However, in late June 2017 the northern copepod anomaly increased from strongly negative to relative neutral values, while the southern copepod anomaly declined from strongly positive to neutral values (Figure 4.1.1). These changes may signal a transition in 2017 from relatively unproductive to average conditions in this region of the CCE. However, the continued presence of warm water at depth (Figure 3.1) and the lack of a dominant northern copepod signal suggest that strong mixing may be required to establish an average or possibly more productive copepod community.

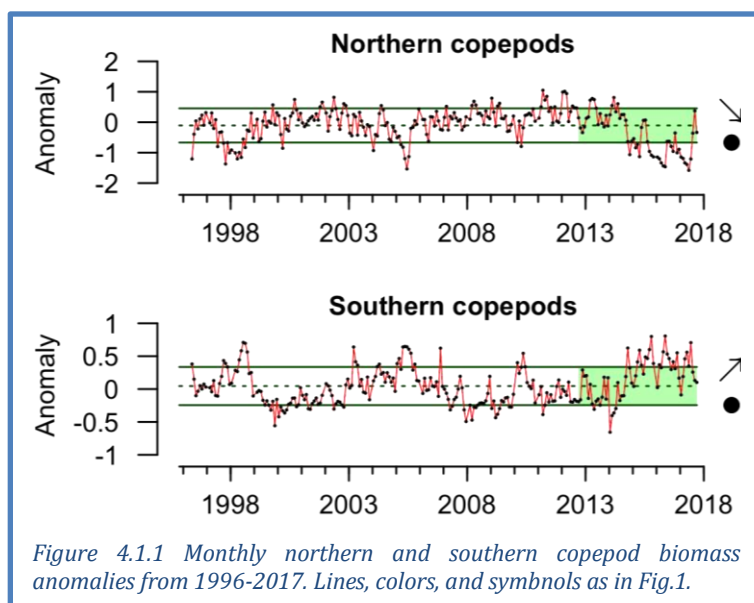


Figure 4.1.1 Monthly northern and southern copepod biomass anomalies from 1996-2017. Lines, colors, and symbols as in Fig.1.

4.2 REGIONAL FORAGE AVAILABILITY

This section describes trends in forage availability, based on research cruises throughout the CCE through spring/summer 2017. These species represent a substantial portion of the available forage in the regions sampled by the cruises (see Figure 2.1c). *We consider these regional indices of relative forage availability and variability, not indices of absolute abundance of coastal pelagic species (CPS).* Absolute abundance estimates should come from stock assessments and comprehensive monitoring programs, which these surveys are not. Moreover, the regional surveys that produce these data use different methods (e.g., gear selectivity, timing, frequency, and survey objectives); thus the amplitudes of each time series are not necessarily comparable between regions.

The CCE forage community is a diverse portfolio of species and life history stages, varying in behavior, energy content, and availability to predators. Years with abundant pelagic fish, market squid and krill are generally associated with cooler waters, strong upwelling and higher productivity (Santora et al. 2014, McClatchie et al. 2016). For space considerations, we present forage indicators as quad plots here; time series plots for each species and region are available in Appendix G.

Northern CCE: The northern CCE survey off Washington and Oregon (see Figure 2.1c) targets juvenile salmon in surface waters, but also catches pelagic fishes, squid, and gelatinous zooplankton. Recent average catches-per-unit-effort (CPUEs) of age 1+ sardine, age 1+ anchovy, market squid and whitebait smelt were within 1 s.d. of long-term means and showed no clear short-term trends (Figure 4.2.1). Sardine and anchovy CPUE were both close to zero (Appendix G, Figure G.1.1). Jack mackerel CPUE has an increasing trend, which continued in 2017, while herring catches have decreased. Also showing a recent decline is a large jellyfish, the sea nettle *Chrysaora*. Finally, extreme numbers of pyrosomes were observed in this region (data not shown). A warm-water gelatinous salp, pyrosomes were common in the 2014-2016 warm events, but catches went up by 10-to 100-fold in 2017 (Brodeur et al. 2018).

Central CCE: Data presented here are from the “Core area” of a survey (see Figure 2.1c) that targets young-of-the-year (YOY) rockfishes, but also samples forage fish, market squid and zooplankton. Adult sardine and anchovy CPUEs were within the long-term range, but remained close to zero in 2017, while YOY rockfish catch was above average for the fifth straight year (Figure 4.2.2; see also Appendix G, Figure G.2.1). Krill and market squid rebounded in 2017 from lower catches in recent years (Appendix G, Figure G.2.1). YOY hake catches have varied widely in recent years, while YOY sanddabs have declined. *Chrysaora* jellyfish have declined

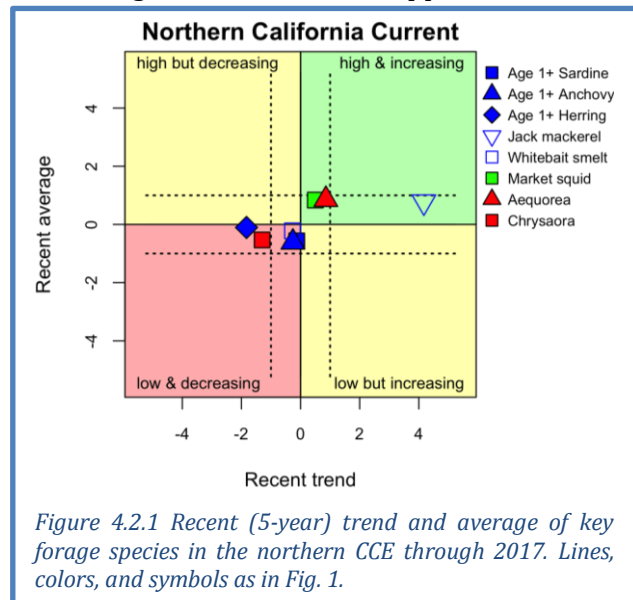


Figure 4.2.1 Recent (5-year) trend and average of key forage species in the northern CCE through 2017. Lines, colors, and symbols as in Fig. 1.

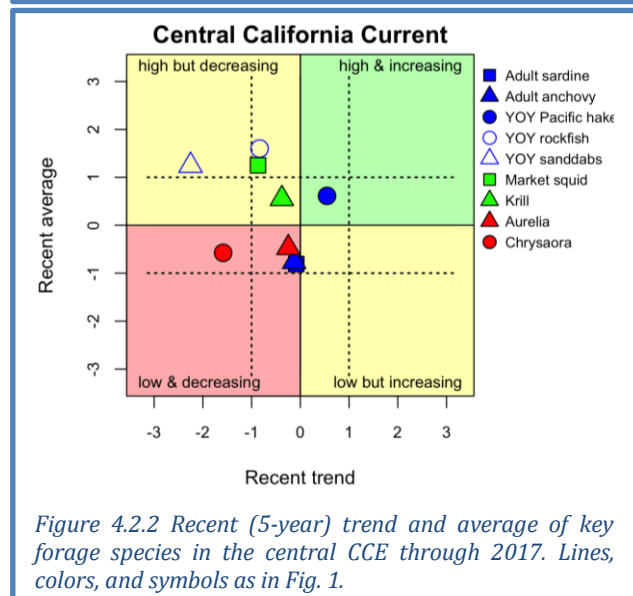


Figure 4.2.2 Recent (5-year) trend and average of key forage species in the central CCE through 2017. Lines, colors, and symbols as in Fig. 1.

recently, though that may be due in part to avoidance of sites where *Chrysaora* has fouled sampling gear in the past. Pyrosomes were relatively abundant in the Central CCE for the fourth year in a row (data not shown).

Southern CCE: Forage indicators for the Southern CCE come from CalCOFI larval fish surveys (see Figure 2.1c). Larval biomass is assumed to correlate with regional abundance of mature forage fish. Recent CPUE for species analyzed through 2017 were within ± 1 s.d. of their long-term means, but several trends are evident (Figure 4.2.3). Larval anchovy and shortbelly rockfish are increasing. Larval sardine CPUE was up slightly in 2017 (Appendix G, Figure G.3.1) but remained nearly 1 s.d. below the long-term average. Larval market squid catches have declined recently and have been very low for the past 3 years. Larval jack mackerel and sanddab catches were close to average in 2017, though both species have declined from strong peaks in recent years.

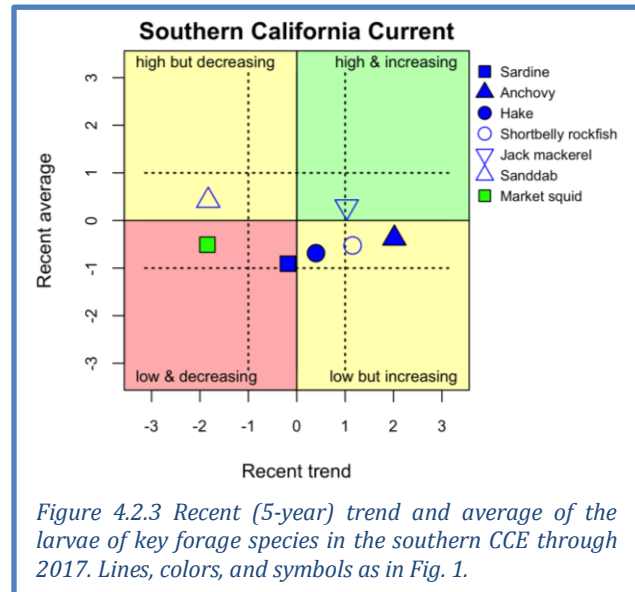


Figure 4.2.3 Recent (5-year) trend and average of the larvae of key forage species in the southern CCE through 2017. Lines, colors, and symbols as in Fig. 1.

4.3 SALMON

For indicators of the abundance of Chinook salmon, we compare the trends in natural spawning escapement from different populations to compare status and coherency in production dynamics across the greater portion of their range. We summarize escapement trends in quad plots; time series are available in Appendix H. We have also added a time series of juvenile salmon catches from a NOAA survey conducted in the Northern CCE off Oregon and Washington (see Figure 2.1c).

Most Chinook salmon escapement data are updated through 2016. Generally, escapements of California Chinook salmon over the most recent decade of data were within 1 s.d. of long-term averages (Figure 4.3.1), although recent escapements were generally near the low end of the normal range (Appendix H, Figure H.1.1). California Chinook salmon stocks have neutral trends over the last decade, and variation in escapement among years is generally relatively high (Appendix H, Figure H.1.1). For Oregon, Washington and Idaho Chinook salmon stocks, most recent escapements were close to average. The exception is Snake River Fall Chinook after a series of large escapements since 2009 (Appendix H Figure H.2.1). Ten-year trends for northern stocks were mostly neutral, but Lower Columbia and Snake River Fall both had significantly positive trends over their most recent decade of escapement data.

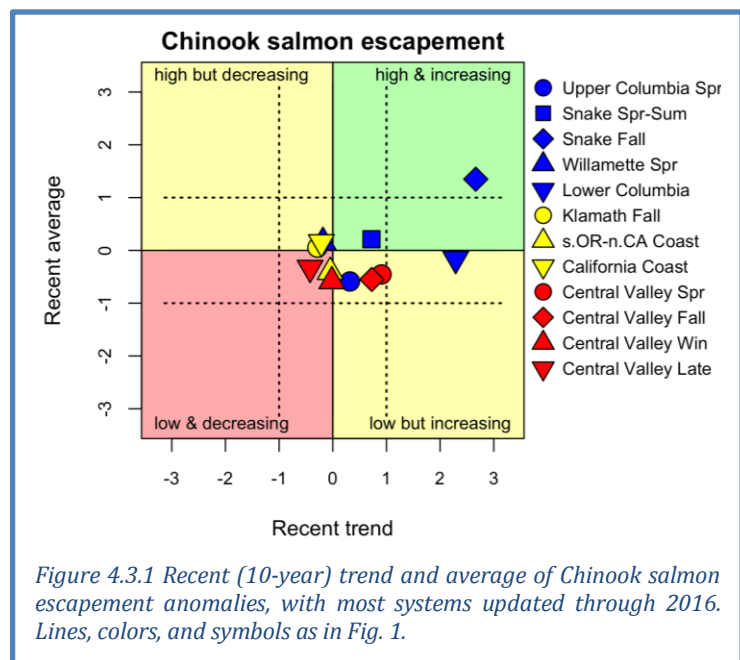
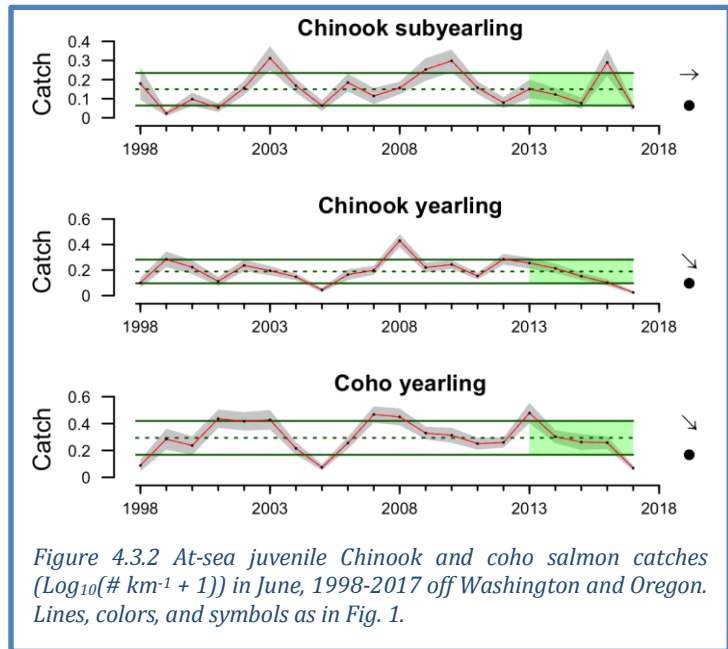


Figure 4.3.1 Recent (10-year) trend and average of Chinook salmon escapement anomalies, with most systems updated through 2016. Lines, colors, and symbols as in Fig. 1.

Catches of juvenile Chinook and coho salmon in June off the coasts of Washington and Oregon can serve as indicators of survival during their early marine phase, and are strongly correlated to later years' returns of adults to Bonneville Dam. Catches of subyearling Chinook, yearling Chinook and yearling coho in 2017 were among the lowest observed since the late 1990s (Figure 4.3.2), suggesting marine conditions in this region continued to be poor for salmon. Yearling Chinook and yearling coho catches have declined over the past 5 years, while subyearling Chinook catches have been more variable.



Many indicators suggest below-average returns will occur for Fall Chinook, Spring Chinook and coho stocks returning to the Columbia Basin in 2018, due in part to lagged effects of the recent warm anomalies in the CCE. NOAA scientists and colleagues are evaluating long-term associations between oceanographic conditions, food web structure, and salmon productivity (e.g., Burke et al. 2013, Peterson et al. 2014). Their assessment is that indicators of conditions for smolts that went to sea between 2014 and 2017 are generally consistent with below-average returns of Chinook and coho salmon to the Columbia Basin in 2018, as depicted in the “stoplight chart” in Table 4.3.1; this includes many indicators in this report, such as PDO, ONI, Copepod Biomass Anomalies and Juvenile Salmon Catch. Recall, too, that the extremely poor freshwater conditions of 2015 (Section 3.4) affected salmon populations during this same smolt year period.

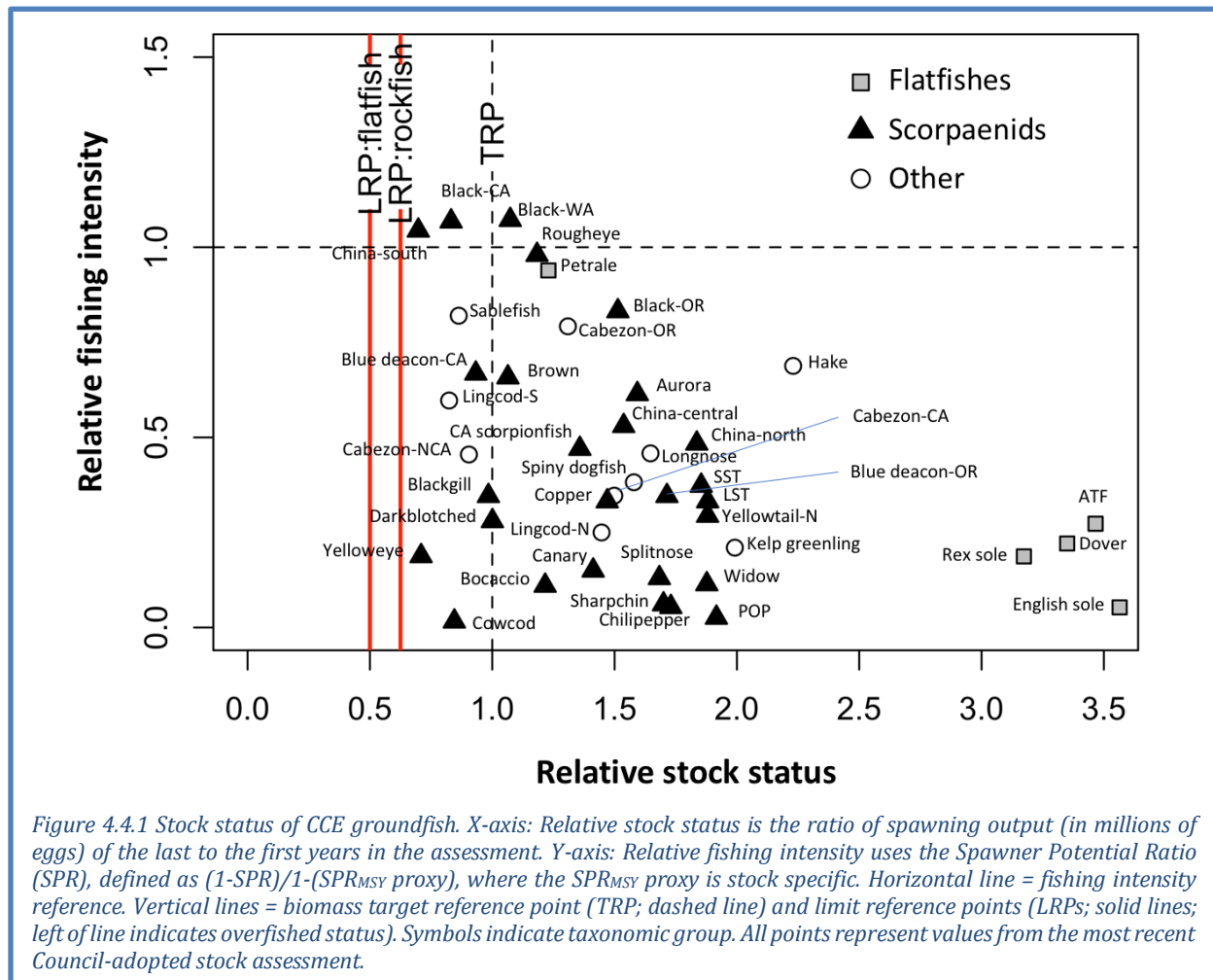
Table 4.3.1 “Stoplight” table of basin-scale and local/regional conditions for smolt years 2014-2017 and likely adult returns in 2018 for coho and Chinook salmon that inhabit coastal Oregon and Washington waters during their marine phase. Green/circles = “good,” i.e., rank in the top third of all years examined. Yellow/squares = “intermediate,” i.e., rank in the middle third of all years examined. Red/diamonds = “poor,” i.e., rank in the bottom third of all years examined. Courtesy of Dr. Brian Burke (NOAA).

Scale of indicators	Smolt year				Adult return outlook	
	2014	2015	2016	2017	Coho, 2018	Chinook, 2018
Basin-scale						
PDO (May-Sept)	Red diamond	Red diamond	Red diamond	Yellow square	Yellow square	Red diamond
ONI (Jan-Jun)	Yellow square	Red diamond	Red diamond	Yellow square	Yellow square	Red diamond
Local and regional						
SST anomalies	Yellow square	Red diamond	Red diamond	Green circle	Green circle	Red diamond
Deep water temp	Red diamond	Red diamond	Yellow square	Red diamond	Red diamond	Yellow square
Deep water salinity	Red diamond	Red diamond	Yellow square	Red diamond	Yellow square	Red diamond
Copepod biodiversity	Yellow square	Red diamond	Red diamond	Yellow square	Yellow square	Red diamond
Northern copepod anomaly	Green circle	Red diamond	Red diamond	Red diamond	Red diamond	Red diamond
Biological spring transition	Yellow square	Red diamond	Red diamond	Red diamond	Red diamond	Red diamond
Winter ichthyoplankton biomass	Red diamond	Green circle	Green circle	Green circle	Green circle	Green circle
Winter ichthyoplankton community	Yellow square	Red diamond	Red diamond	Red diamond	Red diamond	Red diamond
Juvenile Chinook catch (Jun)	Yellow square	Yellow square	Red diamond	Red diamond	Red diamond	Red diamond
Juvenile coho catch (Jun)	Yellow square	Yellow square	Yellow square	Red diamond	Red diamond	Yellow square

4.4 GROUNDFISH: STOCK ABUNDANCE AND COMMUNITY STRUCTURE

The CCIEA team regularly presents the status of groundfish biomass and fishing pressure based on the most recent stock assessments. This year’s report includes updated information from several new assessments in 2017. All groundfishes assessed since 2007 are above the biomass limit reference points (LRPs); thus, no stocks are presently considered “overfished” (Figure 4.4.1, x-axis). While no longer under their LRPs, yelloweye rockfish and cowcod are still rebuilding towards their target biomasses. Three species were declared rebuilt in 2017: bocaccio, darkblotched rockfish and Pacific Ocean perch. Also of note: biomass of arrowtooth flounder (ATF, assessed in 2017) increased sharply from the prior assessment (in 2007). ATF are a predatory species with low market value, and are thought to have predatory impacts on target species in some ecosystems (e.g., Holsman et al. 2016).

Overfishing occurs when catches exceed overfishing limits (OFLs), but not all stocks are managed by OFLs. For summary purposes, our best alternative is to compare fishing rates to proxy rates that are based on a stock’s spawner potential ratio (SPR; Figure 4.4.1, y-axis). Three stocks (black rockfish in California and Washington; China rockfish in California) were being fished above the fishing rate proxy in their most recent assessments (all in 2015).



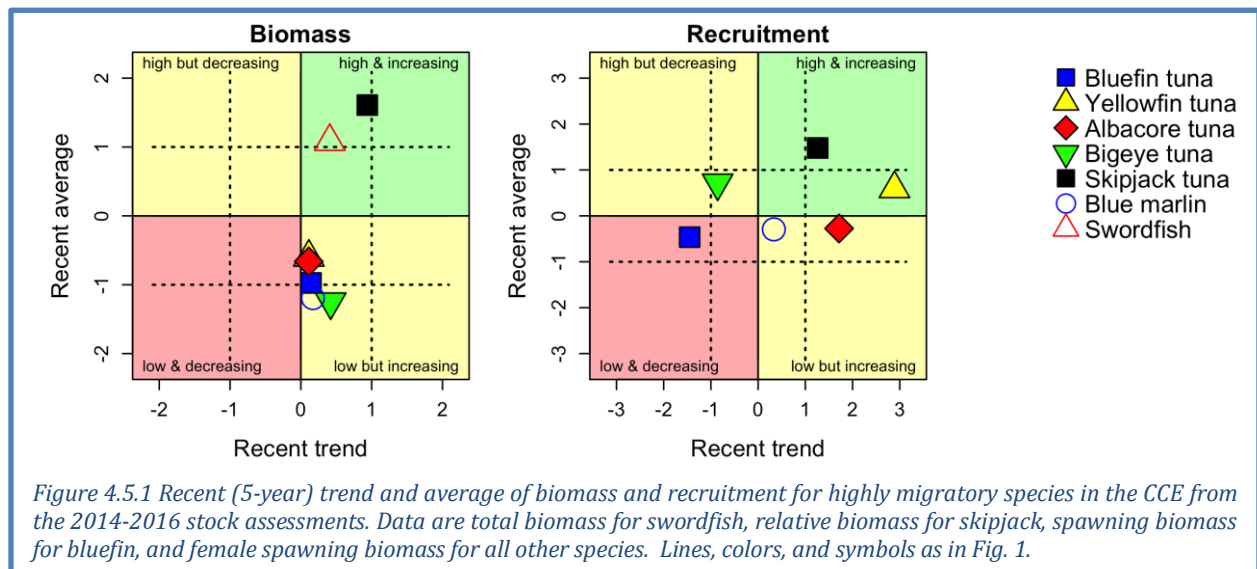
As noted in Section 4.2, YOY rockfish were highly abundant in the Central CCE in 2013-2017, and results from other NOAA surveys also revealed large numbers of pelagic and post-settled juvenile rockfish along the Washington coast in 2016. Given the warm and unproductive conditions of 2014-2016, these findings run counter to what we expected from conceptual models linking climate and

productivity conditions to groundfish populations (see Appendix D, Figure D.2). These rockfish cohorts likely were not yet large enough to have been caught in bottom trawls; thus we will have to wait to determine how groundfish populations respond long-term to the recent climate anomalies.

We are also tracking the abundance of groundfish relative to Dungeness and Tanner crabs as a metric of seafloor community structure. For space considerations, and because the time series are as yet short and difficult to interpret, these indicators are located in Appendix I.

4.5 HIGHLY MIGRATORY SPECIES

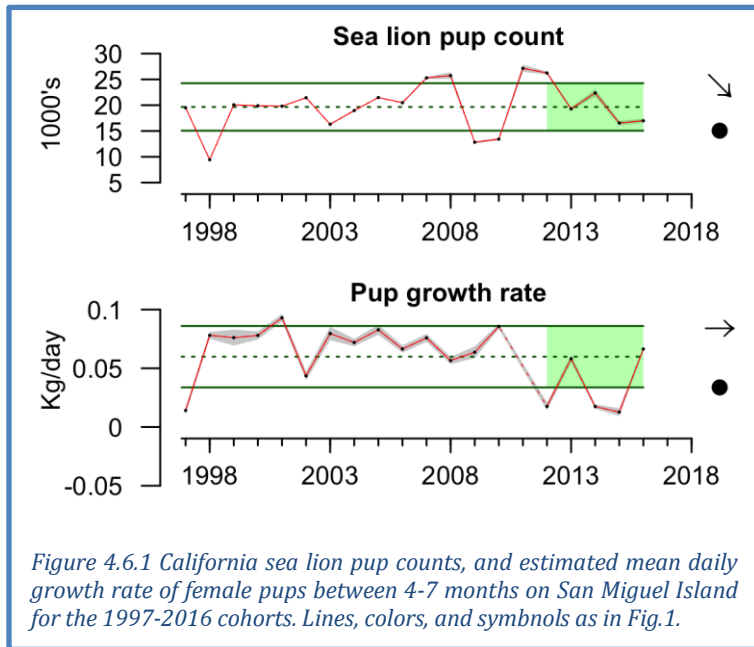
This marks the first year in which we include indicators of highly migratory species (HMS), most of which are managed by the Council. Here we present quad plots of recent averages and trends of biomass and recruitment from the most recent assessments of key HMS target stocks (Figure 4.5.1); time series for these indicators are found in Appendix J, with most recent assessments ranging from 2014-2016. For two stocks (swordfish and skipjack), average biomass over the most recent 5 years was substantially above the long-term average. All other assessed HMS stocks were either within ± 1 s.d. of the average or were below it (e.g., blue marlin, bigeye tuna), and several stocks appeared to be near historic lows (bigeye tuna, bluefin tuna, blue marlin). Biomass trends were statistically neutral for all species, although skipjack may be increasing. Recruitment indicators varied widely: recruitment appears to be increasing for albacore, skipjack and yellowfin tuna, decreasing for bluefin tuna, and neutral for other stocks. The poor numbers for bluefin tuna may be masked by recent high bluefin catches in California, though those catches may be a result of northward and shoreward shifts by bluefin during the anomalous warm years in pursuit of prey (e.g., pelagic red crab) typically found in Baja or offshore. In future CCIEA reports, we hope to add indicators that are related to dynamics and drivers of HMS ecology and distribution.



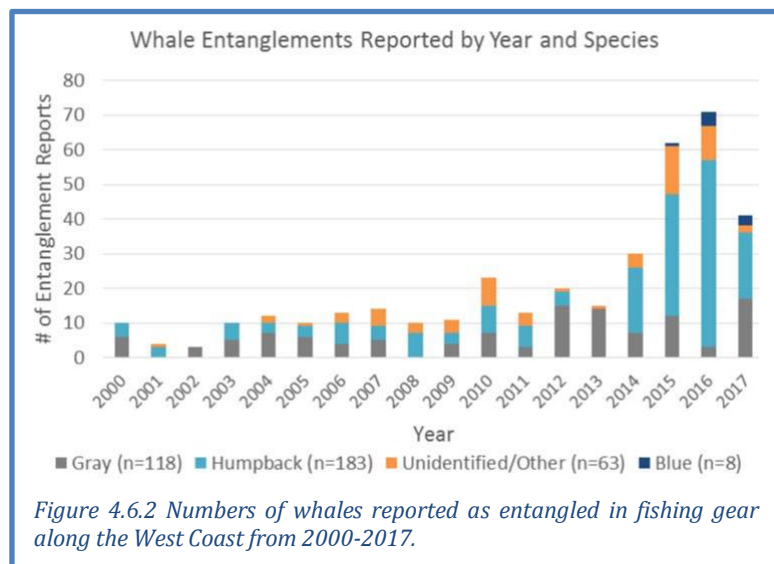
4.6 MARINE MAMMALS

Sea lion production: California sea lions are sensitive indicators of prey availability in the central and southern CCE (Melin et al. 2012): sea lion pup count at San Miguel Island relates to prey availability and nutritional status for adult females from October to June, while pup growth from birth to age 7 months is related to prey availability to adult females during lactation from June to February.

In 2016, pup births at San Miguel Island were below the long-term mean, showing little change from 2015; the trend over the most recent 5 cohorts remained negative (Figure 4.6.1, top). The low numbers of births in 2016 reflect a reduction in the number of reproductive females in the population, due to poor feeding conditions since 2009 (Melin et al. 2012, DeLong et al. 2017). However, growth rates for the 2016 cohort were similar to the long-term average (Figure 4.6.1, bottom), a significant improvement relative to extremely low growth rates of cohorts in 2012, 2014 and 2015. Those same cohorts had experienced unusually high stranding rates, associated with poor foraging conditions for nursing females in the central and southern CCE during the period of pup nutritional dependence (Wells et al. 2013, Leising et al. 2014, Leising et al. 2015, McClatchie et al. 2016). The improved growth of pups in the 2016 cohort indicates that nursing females experienced better foraging conditions during 2016-2017, coinciding with higher frequencies of anchovy and hake in their diets, compared to a diet rich in juvenile rockfish and market squid during the periods of poor survival. If foraging conditions continue to improve, pup survival should also improve, but the effects of poor survival in five of the last seven cohorts will continue to suppress production for several more years.



Whale entanglement: In this year's report, we have added a time series of reported whale entanglements in fixed gears, as a possible indicator of protected species bycatch. Coincident with the anomalous warming of the CCE in 2014-2016, observations of whales entangled in fishing gear occurred at levels far greater than in the preceding decade (Figure 4.6.2). Observed entanglements were most numerous in 2015 and 2016, with the majority involving humpbacks. Most observations occurred in California waters. Based on preliminary data, observed entanglements appeared to decline in 2017, but were still greater than in years from 2000 to 2013. The majority of entanglements occur in gear that cannot be identified visually. Of the portion that can be identified, most appears to be Dungeness crab gear. However, in both 2016 and 2017, sablefish fixed gear was identified in at least one entanglement, and gillnets were observed as entangling gear in 2015, 2016 and 2017. Many interacting factors could be causing the increased numbers of observed



entanglements, including shifts in oceanographic conditions and prey fields that brought the whales closer to shore, as well as changes in distribution and timing of fishing effort; the NOAA West Coast Region will continue to follow this issue as conditions in the CCE change, and the CCIEA team is involved in analyses with researchers from NOAA, other agencies, and academic partners.

4.7 SEABIRDS

Seabird indicators are assumed to reflect regional production and availability of forage, with the three species included here representing distinct feeding strategies to take advantage of the forage portfolio. Sooty shearwaters migrate to the CCE from the southern hemisphere in spring and summer to prey on small fish and zooplankton near the shelf break. Common murres and Cassin’s auklets are resident species that feed over the shelf; Cassin’s auklets prey on zooplankton, while common murres target small fish. For seabird abundance indicators, we use a quad plot to summarize regional time series for at-sea density of three key species during summer; time series are available in Appendix K.

Seabird density patterns varied within and across species. Sooty shearwater densities have undergone significant short-term declines in both the northern and central CCE, and 2017 densities in these regions were among the lowest of the time series (Figure 4.7.1; Appendix K, Figure K.1.1). In sharp contrast, sooty shearwater density in the southern CCE reached its highest recorded density in 2017, continuing a recent, significant short-term increase. Common murre density was slightly below average in the northern CCE, but 2017 common murre densities in the central and southern CCE were the highest ever recorded, resulting in significant short-term increases. Cassin’s auklet density in the northern CCE was above the long-term mean in 2017, but down from a peak in 2015; however, Cassin’s auklet densities were declining in the central CCE and remained just below the long-term mean in the southern CCE.

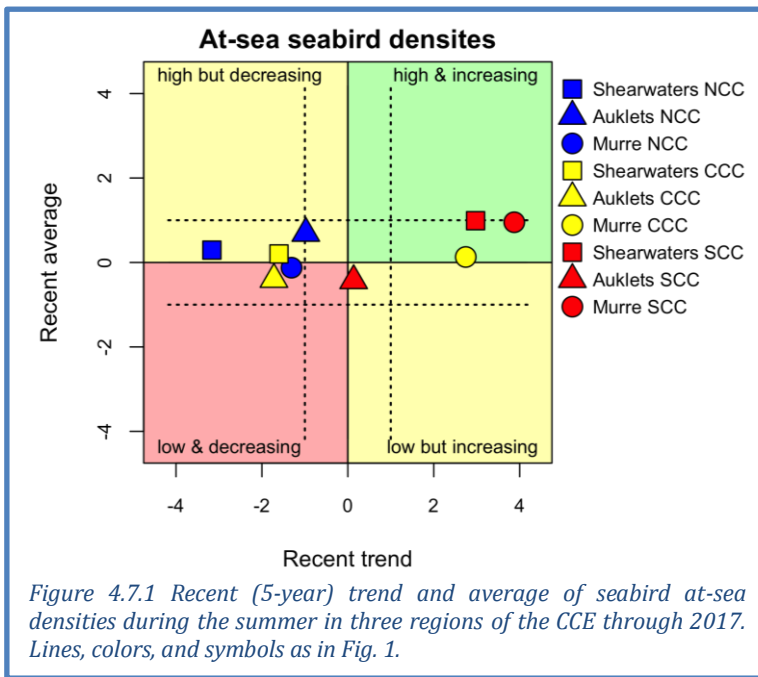


Figure 4.7.1 Recent (5-year) trend and average of seabird at-sea densities during the summer in three regions of the CCE through 2017. Lines, colors, and symbols as in Fig. 1.

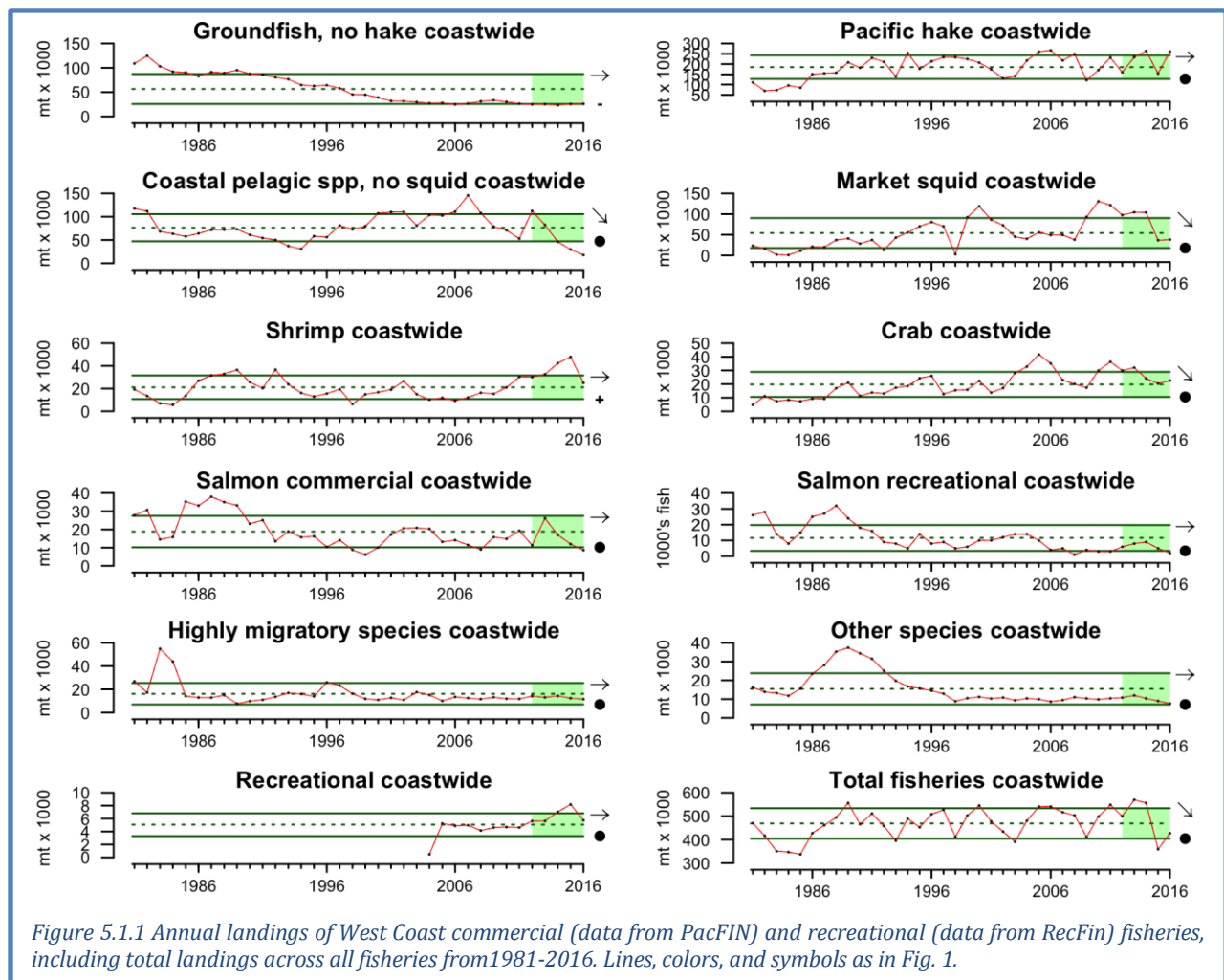
The prior three CCIEA reports from the anomalously warm and unproductive years noted major seabird mortality events in each year. These “wrecks”—exceptional numbers of dead birds washing up on widespread beaches—impacted Cassin’s auklets in 2014, common murres in 2015 and rhinoceros auklets in 2016. In 2017, there were no reports of widespread seabird wrecks related to low productivity; for example, the University of Washington-led Coastal Observation And Seabird Survey Team (COASST) observed average to below-average numbers of beached birds for four index species in 2017 (see Appendix K.3). (Although, we are aware of unpublished reports of localized mortality events in Southern California, possibly related to domoic acid concentrations.)

5 HUMAN ACTIVITIES

5.1 COASTWIDE LANDINGS BY MAJOR FISHERIES

Fishery landings data are current through 2016. Total landings decreased over the last five years,

driven mainly by steep declines in landings of CPS finfish, market squid and crab, along with a large decrease in shrimp landings in 2016 (Figure 5.1.1). Landings of groundfish (excluding hake) were at historically low levels from 2012-2016, while landings of hake were variable. Shrimp landings declined considerably in 2016, but remained at historically high levels from 2012-2016. Commercial landings of salmon were at the lower end of historical levels over the last five years. Landings of HMS and other species have been consistently within ± 1 s.d. of historic averages over the last 20+ years. Methods for sampling and calculating mortality in recreational fisheries changed recently, leading to shorter comparable time series. Recreational landings (excluding salmon and Pacific halibut) were increasing through 2015, but a 70-80% decrease in yellowfin tuna and yellowtail landings in 2016 brought total recreational landings to within historical averages for the last five years (Figure 5.1.1). Landings for recreationally caught Chinook and coho salmon showed no trends and were within historical averages, but any further declines may result in historically low landings in subsequent years. State-by-state commercial and recreational landings are summarized in Appendix L.

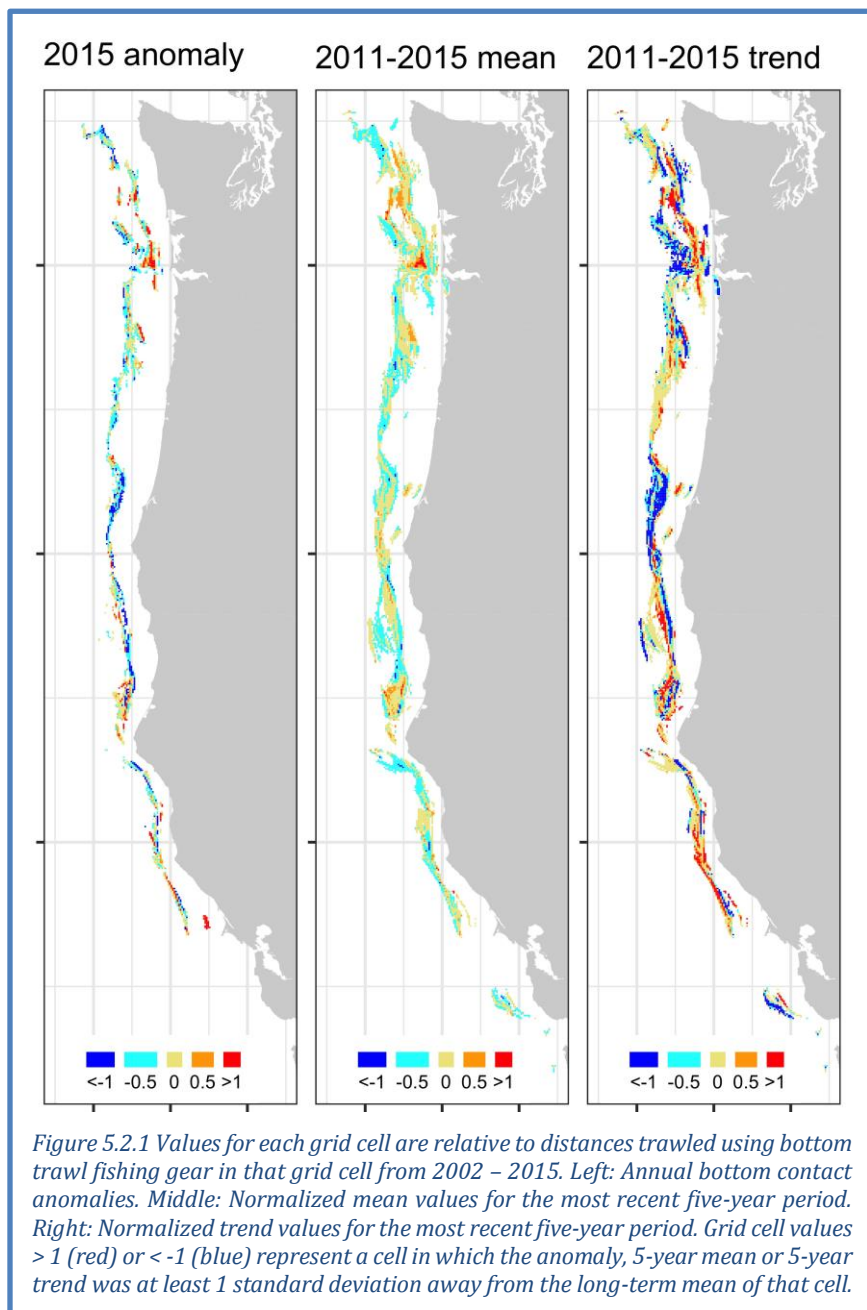


Total revenue across U.S. West Coast commercial fisheries decreased from 2012–2016 (see Appendix L). This decline has been driven primarily by decreases in Pacific hake, CPS finfish, and market squid revenue over the last five years, particularly in 2015. The only fishery that increased in revenue over the last five years was shrimp, although revenue fell dramatically in 2016.

5.2 BOTTOM TRAWL CONTACT WITH SEAFLOOR

Benthic species, communities and habitats can be disturbed by natural processes, and also by human activities (e.g., bottom contact fishing, mining, dredging). The impacts of these activities likely differ by seafloor habitat type, with hard, mixed and biogenic habitats needing longer to recover than soft sediment.

We estimated distance trawled on a 2x2-km grid from 2002-2015. For each grid cell, we mapped the 2015 departure (anomaly) from the long-term mean, the most recent 5-year average and the most recent 5-year trend. For example in 2015, distance trawled was above average for areas off of southern Washington and north of Cape Mendocino, but below average north of Cape Blanco (Figure 5.2.1, left). Red areas in the trend map (Figure 5.2.1, right) indicate large swaths of seafloor off Washington, southern Oregon and northern California where trawl activity increased from 2011-2015, while blue areas off Washington and central Oregon indicate areas where trawl activity declined. Because it highlights status and trends of trawling activity in specific areas, this spatial indicator may be more informative than the time series of the total coastwide distance trawled, which indicates that gear contact with seafloor was at historically low levels and had no trend from 2011-2015 (Appendix M). Subsequent efforts will incorporate other non-fishing human activities that could affect seafloor habitats.



5.3 OTHER HUMAN ACTIVITIES

The CCIEA team compiles and regularly updates indicators of human activities in the CCE, some of

which may have effects on focal species, ecosystem processes and services, fisheries, and coastal communities. Some of these activities relate closely to fisheries (e.g., aquaculture) while others relate to different ocean use sectors like shipping and energy extraction. Several of these time series have recently been updated. For space considerations, we have moved these time series to Appendix N and Appendix O.

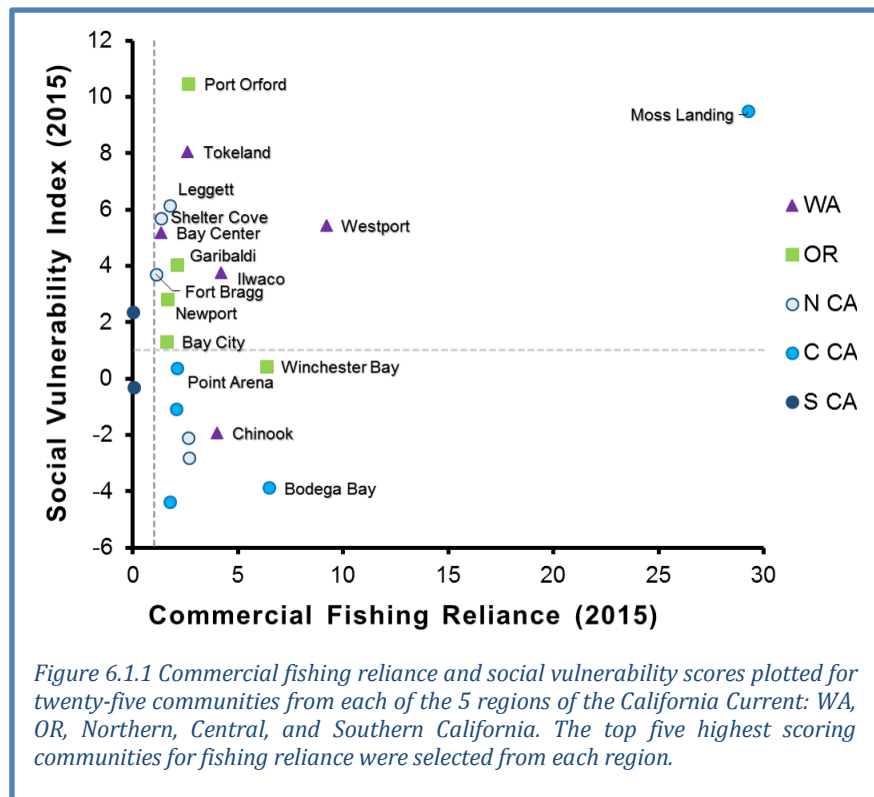
6 HUMAN WELLBEING

6.1 SOCIAL VULNERABILITY

Coastal community vulnerability indices are generalized socioeconomic vulnerability metrics for communities. The Community Social Vulnerability Index (CSVI) is derived from social vulnerability data (demographics, personal disruption, poverty, housing characteristics, housing disruption, labor force structure, natural resource labor force, etc.; see methods in Jepson and Colburn 2013). We monitor CSVI in communities dependent upon commercial fishing (Figure 6.1.1), and in this year's report we add dependence upon recreational fishing (Figure 6.1.2).

The commercial fishing *engagement* index is based on an analysis of variables reflecting commercial fishing engagement in 1140 communities (e.g., fishery landings, revenues, permits, and processing). The commercial fishing *reliance* index applies the same factor analysis approach to these same variables on a per capita basis. Figure 6.1.1 plots CSVI against commercial fishery reliance (per capita dependence) for five communities most dependent on commercial fishing in each of Washington, Oregon, and northern, central and southern California. Of note are communities that are above and to the right of the dashed lines, which indicate 1 s.d. above average levels of social vulnerability (horizontal dashed line) and commercial fishing reliance (vertical dashed line) of all West Coast communities.

For example, both Moss Landing and Westport have high commercial fishing reliance (29 and 9 s.d. above average) and also high CSVI (~10 and 5 s.d. above average). Communities that are strong outliers in both indices may be highly vulnerable to commercial fishing downturns. Shocks due to ecosystem changes or management actions may produce especially high individual and community-level social stress in these communities. As we have discussed in past meetings, these data are difficult to groundtruth and require further study.



The recreational fishing engagement index is based on an analysis of variables reflecting a community’s recreational fishing engagement (e.g., number of boat launches, number of charter boat and fishing guide license holders, number of charter boat trips, and a count of recreational fishing support businesses such as bait and tackle shops). The recreational fishing reliance index applies the same factor analysis approach to these same variables for each community on a per capita basis. Figure 6.1.2 plots CSVI against newly available recreational fishery reliance (again, per capita dependence) for the five communities most heavily dependent on recreational fishing in each of the five geographic regions. Once again, of note are communities that appear above and to the right of the dashed lines, which indicate the 1 s.d. above average levels of recreational reliance (vertical line) and social vulnerability (horizontal line) along the West Coast. Notable communities of this type include Elkton and Westport, although there were fewer communities in this portion of the recreational reliance plot than there were in the commercial reliance plot (Figure 6.1.1). Several communities (Westport, Ilwaco, Garibaldi, Moss Landing) appear in this portion of the plot for both the commercial and recreational sectors, which may imply some potential for management-related tradeoffs in those communities. This is an emerging area of work and more research will be required to understand the importance of these relationships.

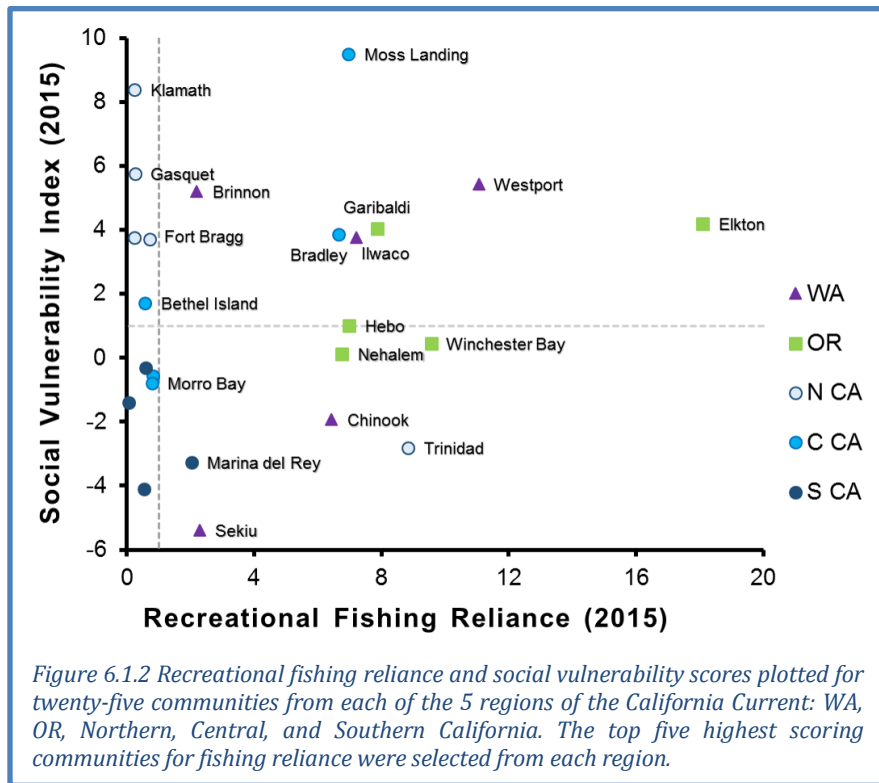


Figure 6.1.2 Recreational fishing reliance and social vulnerability scores plotted for twenty-five communities from each of the 5 regions of the California Current: WA, OR, Northern, Central, and Southern California. The top five highest scoring communities for fishing reliance were selected from each region.

6.2 FLEET DIVERSITY INDICES

Catches and prices from many fisheries exhibit high inter-annual variability leading to high variability in fishermen’s revenue, but variability can be reduced by diversifying fishing activities across multiple fisheries or regions (Kasperski and Holland 2013). We use the effective Shannon index (ESI) to measure diversification among 28,000 fishing vessels on the West Coast and Alaska. The index has an intuitive meaning: ESI = 1 when all revenues are from a single species group and region; ESI = 2 if fishery revenues are spread evenly across 2 fisheries; and so on. It increases both as revenues are spread across *more* fisheries and as revenues are spread more *evenly* across fisheries. If the revenue is not evenly distributed across fisheries, then the ESI value is lower than the number of fisheries a vessel enters.

As of 2016, the fleet of vessels fishing on the West Coast and in Alaska is less diverse on average than at any time in the past 36 years (Figure 6.2.1a). All categories of vessels that fished along the West Coast decreased in average diversification from 2015 to 2016 (Figure 6.2.1b-d). The long term decline is due both to entry and exit of vessels, and to changes for individual vessels. Over time, less

diversified vessels have been more likely to exit; however, vessels that remain in the fishery have also become less diversified, at least since the mid-1990s, and newer entrants have generally been less diversified than earlier entrants. The overall result is a moderate decline in average diversification since the mid-1990s or earlier. Within the average trends, there are wide ranges of diversification levels and strategies within and across vessel classes, and some vessels remain highly diversified. Increased diversification from one year to the next may not always indicate an improvement. For example, if a class of vessels was heavily

dependent on a single fishery with highly variably revenues (e.g., Dungeness crab), a decline in that fishery might force vessels into other fisheries, causing average diversification to increase. Also an increase in a fleet's diversification may be due to the exit of less diversified vessels (Appendix Q).

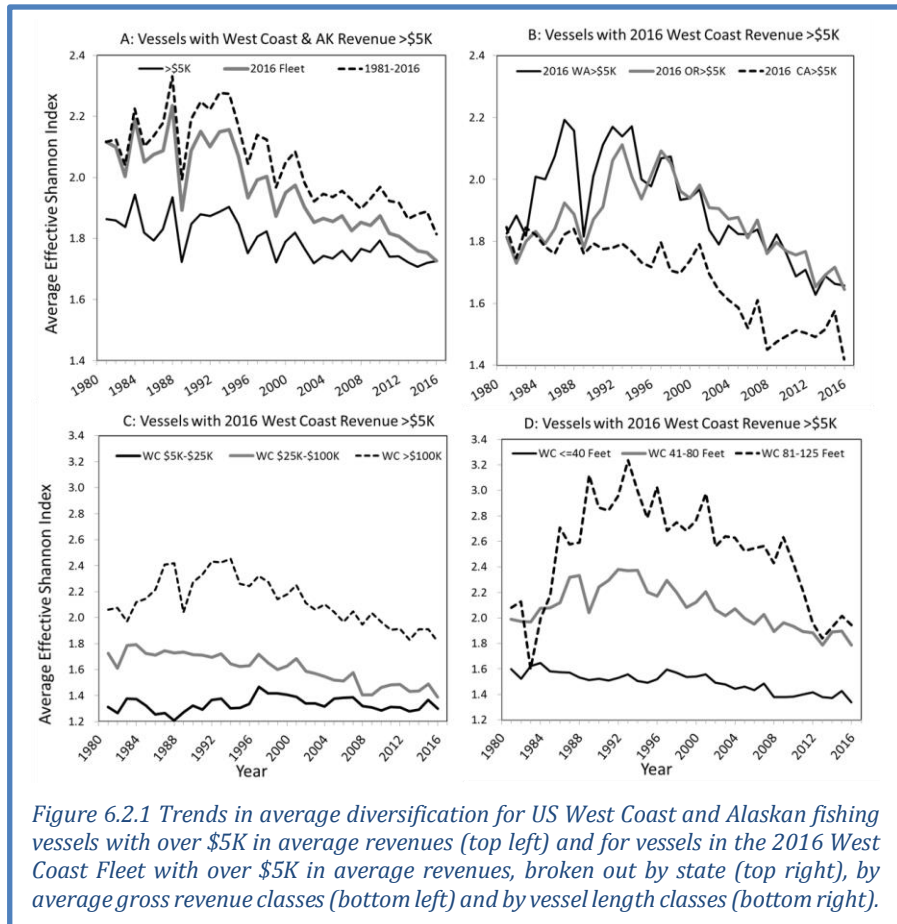


Figure 6.2.1 Trends in average diversification for US West Coast and Alaskan fishing vessels with over \$5K in average revenues (top left) and for vessels in the 2016 West Coast Fleet with over \$5K in average revenues, broken out by state (top right), by average gross revenue classes (bottom left) and by vessel length classes (bottom right).

7 SYNTHESIS

In March 2015, the Council approved FEP Initiative 2, “Coordinated Ecosystem Indicator Review” (Agenda Item E.2.b), by which the Council, advisory bodies, the public, and the CCIEA team would work jointly to refine the indicators in the annual CCIEA Ecosystem Status Report to better meet Council objectives. The Initiative was implemented by an ad-hoc Ecosystem Working Group (EWG). The EWG asked the CCIEA team to include a short section of “Research Recommendations” in the March 2017 California Current Ecosystem Status Report. Those Recommendations are generally consistent with our perspectives on ecosystem research needs in 2018; thus, rather than repeating those recommendations here (see full list in Appendix R), we offer several higher-level analysis products that CCIEA researchers are working on that illustrate several of the 2017 Research Recommendations, and that we hope are of interest to the Council in relation to: (i) continued improvements in this report; (ii) the types of analyses we can provide in other Council contexts, including the new FEP Initiative on Climate and Communities; and (iii) implementation of NOAA Fisheries efforts such as the Ecosystem-Based Fisheries Management Roadmap and the Western Regional Action Plan for the NOAA Climate Science Strategy.

The first two projects (Early Warning Index, Ecosystem Thresholds) relate most closely to Research Recommendations 2 and 3 (Appendix R), and the third project (Dynamic Ocean Management of Bycatch) relates most closely to Research Recommendation 5 (Appendix R).

7.1 AN EARLY WARNING INDEX FOR THE CALIFORNIA CURRENT

In March 2017, the Council requested that the CCIEA team report on the potential for an Early Warning Index to signal major pending changes in the state of the CCE. While past regime shifts in the North Pacific have been associated with sudden changes in the PDO, ecological theory predicts that regime shifts are also to be expected in ecosystems undergoing persistent or incremental perturbations. CCIEA scientists and colleagues used time series data and a family of statistical approaches, reviewed in September 2017 by the SSCES, to look for two indices: (1) an index of the overall ecosystem “state” of both the northern and southern CCE; and (2) an Early Warning Index that would test for impending widespread reorganizations. These methods look for shared, shifting trends in variability across the system as well as for the occurrence of rare “black swan” events that may relate to regime shifts. Preliminary results indicate that current CCE

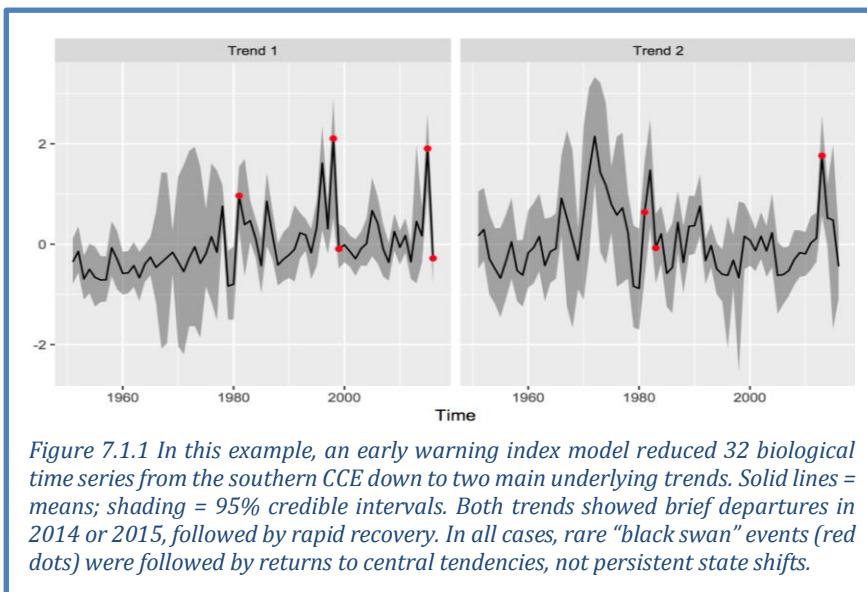


Figure 7.1.1 In this example, an early warning index model reduced 32 biological time series from the southern CCE down to two main underlying trends. Solid lines = means; shading = 95% credible intervals. Both trends showed brief departures in 2014 or 2015, followed by rapid recovery. In all cases, rare “black swan” events (red dots) were followed by returns to central tendencies, not persistent state shifts.

time series show no support for widespread biological reorganization as of 2016, even though the recent climate anomalies of 2014-2016 were near or beyond prior extremes for many variables (Figure 7.1.1). We will continue to revisit these analyses as time series in the CCE add further data.

7.2 IDENTIFYING ECOSYSTEM THRESHOLDS IN INDICATORS

We are examining relationships between indicators of pressures and indicators of key species or processes in the CCE to determine if there are thresholds beyond which a pressure could have much stronger impacts on some part of the system. These thresholds may represent ecosystem reference points that are deserving of management attention in the future. One case study from this project, which was reviewed by the SSCES in September 2017 and recently published (Samhuri et al. 2017), was a threshold relationship between California sea lion pup counts and a large-scale oceanographic metric called the Northern Oscillation Index (NOI), which is an indicator of atmospheric processes that affect upwelling. As shown in Figure 7.2.1, sea lion pup production drops dramatically when summer NOI increases beyond a value of ~0.2,

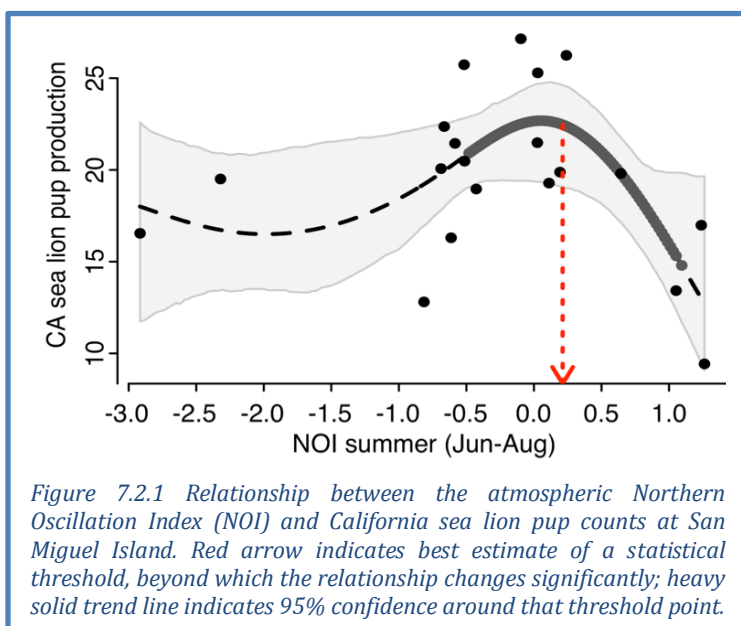


Figure 7.2.1 Relationship between the atmospheric Northern Oscillation Index (NOI) and California sea lion pup counts at San Miguel Island. Red arrow indicates best estimate of a statistical threshold, beyond which the relationship changes significantly; heavy solid trend line indicates 95% confidence around that threshold point.

based on data from 1996-2016. Many ecological time series in the CCE are just reaching a duration that allows for robust time series analyses like these, and the CCIEA team will test for other such thresholds in the near future. In particular, we will be looking at potential threshold responses by salmon populations to natural and anthropogenic pressures.

7.3 DYNAMIC OCEAN MANAGEMENT OF BYCATCH IN THE DRIFT GILLNET FISHERY

CCIEA scientists, with support from NASA, are supporting a risk analysis for bycatch species in the California Drift Gillnet fishery. This fishery is heavily managed to reduce leatherback and loggerhead sea turtle bycatch due to their endangered status, yet large-scale seasonal closures of swordfish fishing are the primary tool for avoiding bycatch. To address this, the team created the EcoCast product (<http://oceanview.pfeg.noaa.gov/ecocast/>), which assesses likelihood of catching swordfish relative to bycatch species in near-real time. Risk weightings were determined based on discussions with managers; leatherback turtles had the highest risk weighting among protected species included. EcoCast is available for fishery participants to inform their decisions on where and when to fish. In addition, the tool can be used to evaluate the recent warm anomalies relative to past, more normal conditions (Figure 7.3.1). The predictive model was used to examine how large, dynamically managed areas would compare to existing seasonal closures under different scenarios; for example, Figure 7.3.1 (left) was a very conservative scenario to protect the top 75% of predicted leatherback habitat, while Figure 7.3.1 (right) was a less-conservative scenario to protect the top 50% of combined EcoCast risk surfaces across turtles, pinnipeds and blue sharks. Of note, 2015 showed increased areas of high risk particularly late in the season compared to 2012. With the development of seasonal forecasting and climate-predicting ocean models, this tool could be used to proactively assess likely fishing conditions for use by the fishery.

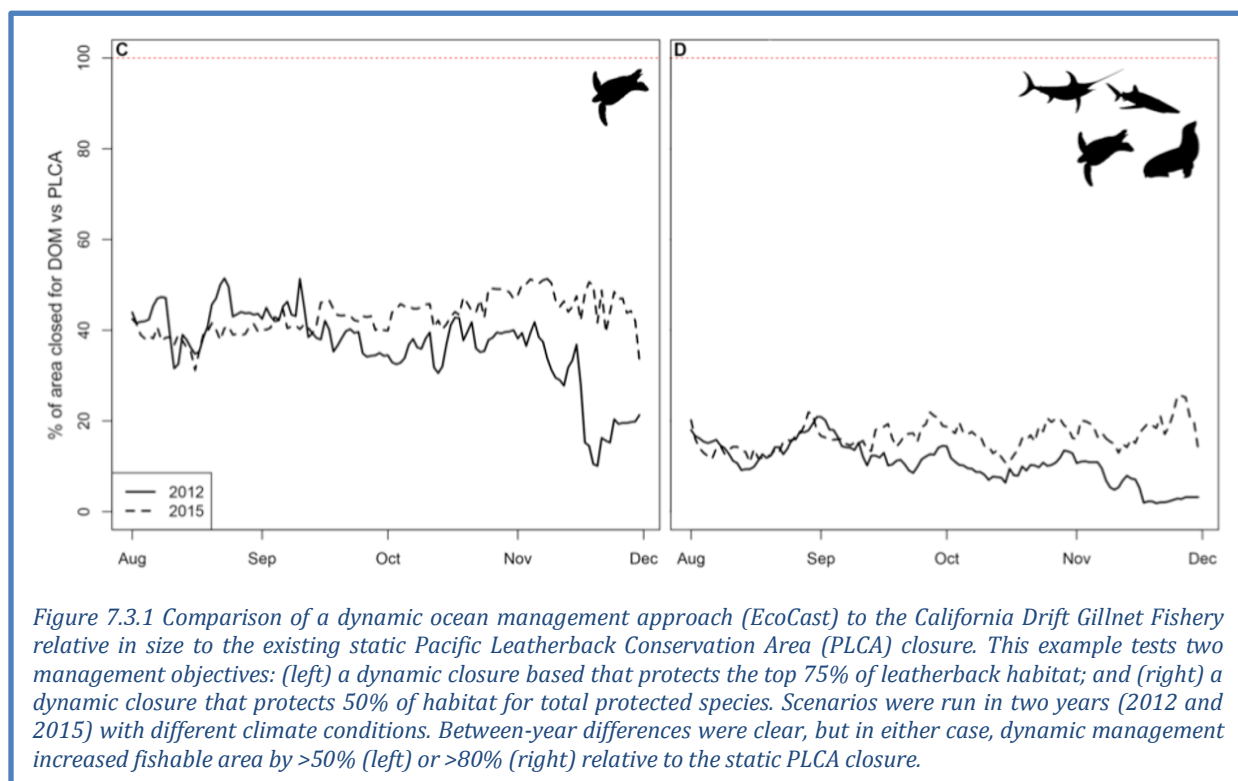


Figure 7.3.1 Comparison of a dynamic ocean management approach (EcoCast) to the California Drift Gillnet Fishery relative in size to the existing static Pacific Leatherback Conservation Area (PLCA) closure. This example tests two management objectives: (left) a dynamic closure based that protects the top 75% of leatherback habitat; and (right) a dynamic closure that protects 50% of habitat for total protected species. Scenarios were run in two years (2012 and 2015) with different climate conditions. Between-year differences were clear, but in either case, dynamic management increased fishable area by >50% (left) or >80% (right) relative to the static PLCA closure.